

## FOR PEER REVIEW - CONFIDENTIAL

### **Facies Interpretation and Geochronology of Diverse Eocene Floras and Faunas, Northwest Chubut Province, Patagonia, Argentina**

**Tracking no:** B35611R

**Authors:**

Justin Gosses, Alan Carroll (University of Wisconsin), Benjamin Bruck (University of Wisconsin-Madison), Brad Singer (University of Wisconsin-Madison), Brian Jicha (University of Wisconsin - Madison), Eugenio Aragón (Universidad Nacional de La Plata), Andrew Walters (University of Wisconsin-Madison), and Peter Wilf (Pennsylvania State University)

**Abstract:**

The Eocene La Huirera Formation of northwestern Patagonia, Argentina, is renowned for its diverse, informative, and outstandingly preserved fossil biotas. In northwest Chubut Province, this unit includes one of the most diverse fossil floras known from the Eocene, as well as significant fossil insects and vertebrates, at the Laguna del Hunco locality. It also includes rich fossil vertebrate faunas at the Laguna Fría and La Barda localities. Previous studies of these important occurrences have provided relatively little sedimentological detail, and radiotopic age constraints are relatively sparse and in some cases obsolete. Here we describe five fossiliferous lithofacies deposited in four terrestrial depositional environments: lacustrine basin-floor, subaerial pyroclastic plain, vegetated, waterlogged pyroclastic lake margin, and extra-caldera incised valley. The best fossil preservation is interpreted to result from the favorable intersection of multiple taphonomic factors, such as rapid input of biological remains, lakewater anoxia, and rapid burial by volcanic ash. We also report several new 40Ar/39Ar age determinations. Among these, the uppermost unit of the caldera-forming Ignimbrita Barda Colorado yielded an 40Ar/39Ar age of 52.54 {plus minus} 0.17 Ma, ~6 Ma younger than previous estimates and demonstrating that fossiliferous lacustrine deposition (previously constrained to > 52.22 {plus minus} 0.22 Ma) must have begun almost immediately on the subsiding ignimbrite surface. A minimum age for Laguna del Hunco fossils is established by an overlying ignimbrite with an age 49.19 {plus minus} 0.24, confirming that deposition took place during the Early Eocene Climatic Optimum. The Laguna Fría mammalian fauna is younger, constrained between a valley-filling ignimbrite and a capping basalt with 40Ar/39Ar ages of 49.26 {plus minus} 0.30 Ma and 43.50 {plus minus} 1.14 Ma, respectively. The latter age is ~4 Ma younger than previously reported. These new ages more precisely define the age range of the Laguna Fría and La Barda fauna, allowing greatly improved understanding of its position with respect to South American mammal evolution, climate change, and geographic isolation.

# 1 *Facies Interpretation and Geochronology of Diverse Eocene Floras and Faunas,*

2 *Northwest Chubut Province, Patagonia, Argentina*

3  
4 **Justin Gosses<sup>1†</sup>, Alan R. Carroll<sup>1</sup>, Benjamin T. Bruck<sup>1</sup>, Brad S. Singer<sup>1</sup>, Brian R. Jicha<sup>1</sup>, Eugenio**  
5 **Aragón<sup>2</sup>, Andrew P. Walters<sup>1</sup> Peter Wilf<sup>3</sup>,**

6

*7      <sup>1</sup>Department of Geoscience, University of Wisconsin – Madison, 1215 W. Dayton St., Madison,  
8      Wisconsin 53706, USA*

<sup>9</sup> *<sup>2</sup>CONICET–Centro de Investigaciones Geológicas, Universidad Nacional de la Plata, B1900FWA La*  
<sup>10</sup> *Plata, Argentina*

11 <sup>3</sup>*Department of Geosciences, Pennsylvania State University, University Park, Pennsylvania 16802,*  
12 *USA*

<sup>†</sup> Present address: Office of the Chief Information Officer, NASA Johnson Space Center, 2101 NASA Parkway, Houston, Texas 77058

15

16

## 17 ABSTRACT

18 The Eocene Huitrera Formation of northwestern Patagonia, Argentina, is renowned for its  
19 diverse, informative, and outstandingly preserved fossil biotas. In northwest Chubut Province, this unit  
20 includes one of the most diverse fossil floras known from the Eocene, as well as significant fossil  
21 insects and vertebrates, at the Laguna del Hunco locality. It also includes rich fossil vertebrate faunas at  
22 the Laguna Fría and La Barda localities. Previous studies of these important occurrences have  
23 provided relatively little sedimentological detail, and radiotopic age constraints are relatively sparse  
24 and in some cases obsolete. Here we describe five fossiliferous lithofacies deposited in four terrestrial  
25 depositional environments: lacustrine basin-floor, subaerial pyroclastic plain, vegetated, waterlogged  
26 pyroclastic lake margin, and extra-caldera incised valley. We also report several new  $^{40}\text{Ar}/^{39}\text{Ar}$  age

27 determinations. Among these, the uppermost unit of the caldera-forming Ignimbrita Barda Colorada  
28 yielded an  $^{40}\text{Ar}/^{39}\text{Ar}$  age of  $52.54 \pm 0.17$  Ma, ~6 Ma younger than previous estimates and  
29 demonstrating that deposition of overlying fossiliferous lacustrine strata (previously constrained to  $>$   
30  $52.22 \pm 0.22$  Ma) must have begun almost immediately on the subsiding ignimbrite surface. A  
31 minimum age for Laguna del Hunco fossils is established by an overlying ignimbrite with an age  $49.19$   
32  $\pm 0.24$ , confirming that deposition took place during the Early Eocene Climatic Optimum. The Laguna  
33 Fría mammalian fauna is younger, constrained between a valley-filling ignimbrite and a capping basalt  
34 with  $^{40}\text{Ar}/^{39}\text{Ar}$  ages of  $49.26 \pm 0.30$  Ma and  $43.50 \pm 1.14$  Ma, respectively. The latter age is ~4 Ma  
35 younger than previously reported. These new ages more precisely define the age range of the Laguna  
36 Fría and La Barda faunas, allowing greatly improved understanding of their positions with respect to  
37 South American mammal evolution, climate change, and geographic isolation.

38

## 39 INTRODUCTION

40 The Patagonian region of Argentina holds historic and still rapidly-expanding significance for  
41 understanding the evolution and biogeography of terrestrial life in the Southern Hemisphere (e.g.,  
42 Ameghino, 1906; Gaudry, 1906; Simpson, 1980; Archangelsky, 2005; Pascual, 2006; Salgado, 2007).  
43 In recent years, there has been a marked increase in investigations of early Paleogene strata, which hold  
44 vital and still little-studied records of recovery from the end-Cretaceous extinction, biotic responses to  
45 climate changes, and biogeographic events related to the final breakup of Gondwana and the beginning  
46 of South American isolation ( e.g., see summaries by Goin et al., 2012a; Wilf et al., 2013).

47 Fundamental to the rising significance of Patagonia's outstanding fossils is the increase in  
48 stratigraphic and sedimentological studies that give the fossiliferous strata geologic context, including  
49 high-precision radioisotopic ages and paleomagnetic data. In just the past few years, a high-resolution  
50 temporal and general geologic framework has emerged for the classic, extremely fossiliferous

51 Paleocene to Miocene continental sequence of southern Chubut Province (Bellosi, 2010; Dunn et al.,  
52 2013; Clyde et al., 2014; Woodburne et al., 2014; Comer et al., 2015; Krause et al., 2017). These data  
53 constrain interpretations for a large variety of studies, from those on individual fossil sites and taxa to  
54 reinterpretations of mammalian evolutionary faunas and their biozonations, known as South American  
55 Land Mammal “Ages” (SALMAs) (Flynn and Swisher, 1995; Gelfo et al., 2009; Woodburne et al.,  
56 2014a,b).

57 Our focus here is on another highly fossiliferous area, in northwest Chubut Province, known as  
58 the Middle Chubut River Pyroclastic and Volcanic Complex of the Huirera Formation (Fig. 1; Aragón  
59 and Romero, 1984; Mazzoni et al., 1991; Aragón and Mazzoni, 1997; Aragón et al., 2001, 2004, 2018).  
60 The Piedra Parada caldera preserves diverse Eocene volcanic rocks, including the caldera-floor  
61 sIgnimbrita Barda Colorada (IBC), a caldera-filling lacustrine sequence known as the Tufolitas Laguna  
62 del Hunco, at least two youger ignimbrite units, and a succession of capping volcanic rocks of the  
63 Andesitas Huancache (Archangelsky, 1974; Mazzoni et al., 1989; Aragón and Mazzoni, 1997; Mazzoni  
64 et al. 1991; Figs. 1, 2).

65 The fossil richness and significance of the Tufolitas Laguna del Hunco has been well known  
66 since Berry’s (1925) first report of the fossil flora from the principal section at Laguna del Hunco in the  
67 northeasternmost exposures of the Tufolitas (Fig. 1). This was followed over several decades by  
68 publications on fossil plants (e.g., Frenguelli, 1943; Romero and Hickey, 1976; Romero et al., 1988),  
69 insects (Fidalgo and Smith, 1987), catfish (Dolgopol de Sáez, 1941; Azpelicueta and Cione, 2011), and  
70 pipoid frogs (Casamiquela, 1961; Báez and Trueb, 1997). Over the past 15 years there has been a  
71 marked increase in research activity on these strata, fueled by renewed, stratigraphically controlled  
72 collecting efforts that have recovered many thousands of specimens (Wilf et al., 2003; Wilf et al.,  
73 2005a). Initial phases of this work revealed that the Laguna del Hunco flora is among the most diverse  
74 from the Eocene worldwide, currently containing more than 200 species (Wilf et al., 2003, 2005a,

75 2005b). Systematic studies have detailed numerous, novel records of diverse plant genera that live  
76 today only in Old World rainforests of Australasia and SE Asia; many of these taxa were previously  
77 only known as fossils, if at all, in Australia and New Zealand. These records, and accompanying  
78 reports of new fossil insects (e.g., Petrulevičius and Nel, 2013; Petrulevičius, 2016 ), are far too  
79 numerous to cite completely here (for summaries see Wilf et al., 2009; Wilf et al., 2013; Kooyman et  
80 al., 2014). However, among the most remarkable discoveries are the outstanding fossils of kauris  
81 (*Agathis*, Araucariaceae), gums (*Eucalyptus*, Myrtaceae), tomatillos (*Physalis*, Solanaceae), and beech  
82 relatives (*Castanopsis*, Fagaceae) (Gandolfo et al., 2011; Wilf et al., 2014, 2017)(Wilf et al., 2019).  
83 The fossil plants from Laguna del Hunco have revealed Eocene Patagonia as the western end of a trans-  
84 Antarctic rainforest biome that harbored elevated biodiversity that was largely lost to extinction  
85 following Antarctic separation and climate change (e.g., Kooyman et al., 2014). In addition, the ages of  
86 many fossil plant lineages from Laguna del Hunco are significantly older than comparable molecular-  
87 clock estimates, challenging that widely-used methodology (Wilf and Escapa, 2015; Wilf et al., 2017).

88 The fossil richness of the study area also includes a pair of rich Eocene mammalian faunas, the  
89 Laguna Fría and La Barda assemblages, that occur within valley-fill deposits (Fig. 1). These faunas  
90 were first collected by R. Pascual in the 1950s and have been the topic of intense study (Goin et al.,  
91 2000, 2001; Tejedor et al., 2005; Tejedor et al., 2009; Lorente et al., 2016). Together, these sites have  
92 produced more than 50 mammalian species, including the oldest South American bats (Tejedor et al.,  
93 2005), the last occurrence of South American gondwanatheres (Goin et al., 2012b), and a diverse array  
94 of other marsupial and placental taxa, especially xenarthrans and ungulates (Tejedor et al., 2009;  
95 Lorente, 2016; Lorente et al., 2016). These faunas, often referred to collectively as the Paso del Sapo  
96 fauna (after the nearby village of the same name; Fig. 1), are noted for their familial affinities with  
97 middle Eocene Antarctic Peninsula faunas of the La Meseta Formation (e.g., Goin et al., 1999; Reguero  
98 et al., 2013; Reguero et al., 2014; Goin et al., 2018). In addition, some marsupial remains have been

99 assigned to the australidelphid clade (Lorente et al., 2016), which includes all living Australian  
100 marsupials and one South American species. Thus, along with the celebrated Danian monotremes from  
101 southern Chubut (Pascual et al., 1992), the Laguna Fría and La Barda faunas provide some of the  
102 firmest evidence for a Gondwanic biogeographic signal in South America's early Paleogene mammals.  
103 These discoveries parallel abundant data from non-mammalian vertebrate groups and plants (e.g., Wilf  
104 et al., 2013 for summary) and modern paleogeographic data (e.g., Lawver et al., 2011) and contrast  
105 with the classic portrayal of South America as an isolated “island continent” for most of the Cenozoic  
106 (Simpson, 1950; Simpson, 1980).

107 Despite the broad significance of the Laguna Fría and La Barda faunas, three issues surround  
108 the interpretation of their age, hindering a precise understanding of their position in the evolutionary  
109 sequence represented in the SALMA scheme. First, Tejedor et al. (2009; also Woodburne et al., 2014a,  
110 b; Goin et al., 2018) proposed that the Laguna Fría and La Barda faunas are, collectively,  
111 compositionally and temporally distinct, falling in an otherwise undocumented “Sapoan” provisional  
112 SALMA between putatively older Río Chican and younger Vacan faunas. The “Sapoan” concept is  
113 widely used, having been followed by all the subsequent workers treating these faunas (citations  
114 above). However, the assessment of geologic age of the faunas (Tejedor et al., 2009) was based on a set  
115 of unpublished  $^{40}\text{Ar}/^{39}\text{Ar}$  dates from a conference abstract reporting the M.S. thesis results of the  
116 present lead author (Gosses, 2006; Gosses et al., 2006), as well as uncertain correlations to now-  
117 obsolete, whole-rock K-Ar dates on basalts exposed elsewhere (e.g., Mazzoni et al., 1991). We, like  
118 Krause et al. (2017), emphasize that the critical  $^{40}\text{Ar}/^{39}\text{Ar}$  ages (Gosses et al., 2006) used by Tejedor et  
119 al. (2009) and subsequent workers have not, until now, been vetted, revised, or reanalyzed. Second,  
120 Laguna Fría and La Barda could be separated enough in time that at least one assemblage temporally  
121 overlaps previously defined SALMAs (Krause et al., 2017). Third, and beyond the scope of the present  
122 study, is that the temporal bounds of the Río Chican SALMA used for comparison are not well

123 established because the type Río Chican mammal sites (Simpson, 1935) have not been placed in a  
124 modern chronostratigraphic framework (Krause et al., 2017). Further, based on a series of new high-  
125 precision U-Pb ages from the Koluel Kaike Formation of southern Chubut Province, which is  
126 traditionally but perhaps incorrectly correlated with the type Río Chican, the Río Chican SALMA is  
127 likely to temporally overlap both the Vacan and the La Barda faunas (Krause et al., 2017).

128 Throughout the study area, reliable stratigraphy that directly constrains the ages of closely  
129 associated fossils is, so far, only established at Laguna del Hunco itself (see Previous Geochronology).  
130 The Laguna Fría and La Barda faunas are only loosely constrained by a set of obsolete K-Ar age  
131 determinations of associated volcanic rocks (Archangelsky, 1974; Mazzoni et al., 1991), excepting the  
132 use by Tejedor et al. (2005; 2009) of then-unpublished initial geochronologic data, including those of  
133 Gosses (2006), which are revised and formally presented here. Several whole-rock K-Ar ages for other  
134 units in the volcanic complex were also pioneering for their time but, likewise, used now-obsolete  
135 techniques with very large uncertainties (Mazzoni et al., 1991). Similarly, important earlier work on the  
136 depositional environments and processes that preserved the fossils (Petersen, 1946; Feruglio, 1949;  
137 Aragón and Romero, 1984; Aragón and Mazzoni, 1997) requires updating from new methods and field  
138 observations.

139 In this study, the depositional histories of five fossil-bearing lithofacies are examined to gain  
140 insights into volcano-sedimentary evolution across the study area (Fig. 1).  $^{40}\text{Ar}/^{39}\text{Ar}$  geochronology is  
141 used to improve chronostratigraphic resolution of the uppermost Ignimbrita Barda Colorada, the strata  
142 holding the Laguna Fría fauna, and other localities. New age determinations for the Ignimbrita Barda  
143 Colorada help to establish the duration of time between the cessation of primary caldera eruption and  
144 fossiliferous lacustrine deposition of the Tufolitas Laguna del Hunco. Other ages permit improved  
145 understanding of the temporal and geographic evolution of the globally significant caldera fossil-lake

146 system and establish reliable constraints for the Laguna Fría fauna that will allow it to be placed  
147 correctly in the SALMA biozonation.

148

149 **GEOLOGIC SETTING**

150 The Tufolitas Laguna del Hunco infill the Piedra Parada caldera within the Eocene Middle  
151 Chubut River Pyroclastic and Volcanic Complex of the La Huitrera Formation (Aragón and Romero,  
152 1984; Aragón and Mazzoni, 1997; Aragón et al., 2004). The complex occurs along a line of Eocene  
153 volcanic centers, referred to as the Pilcaniyeu belt, that stretch in a north-south direction and lie ~150  
154 km east of modern arc volcanism (Rapela et al., 1984; Franzese, 1987; Rapela et al., 1988; Iannelli et  
155 al., 2017). Many outstanding fossil sites are located elsewhere in the Pilcaniyeu belt, especially in the  
156 western exposures near San Carlos de Bariloche in Río Negro (Berry, 1938; Aragón and Romero,  
157 1984; Báez and Pugener, 2003; Melendi et al., 2003; Barreda et al., 2010; Wilf et al., 2010;  
158 Petrulevičius, 2015). The Piedra Parada caldera is trapdoor style (cf., Lipman, 1997), extends 25-30  
159 kilometers N-S, and is located in northwestern Chubut Province, Argentina (Fig. 1). The caldera-  
160 forming ignimbrite, known as the Ignimbrita Barada Colorada (IBC), is overlain by the Tufolitas  
161 Laguna del Hunco, which consists mainly of sub-aerial and lacustrine ash and lapilli that are variably  
162 reworked with a smaller amount of interbedded lava flows and glass domes (Aragon and Mazzoni,  
163 1997). Outcropping strata are as thick as 400 m, with the basal contact often not exposed. Nearly all  
164 published fossils from the Tufolitas Laguna del Hunco (cited earlier) come from the principal section at  
165 Laguna del Hunco, in the northeasternmost exposures (Fig. 1), but recent discoveries are emerging  
166 from the southern outcrops as well (Bippus et al., 2016, 2019; Bomfleur and Escapa, 2019).

167 Above the Tufolitas Laguna del Hunco, capping deposits extend past the caldera edge and  
168 consist of lava flows and dikes but few pyroclastic or sedimentary deposits. The Huancache and Cerro  
169 Mirador Formations are some of the capping units. The Laguna Fría fauna (Figs. 1, 2; citations above)

170 is found within a paleo-valley that was incised into the caldera-forming ignimbrite external to the  
171 caldera itself and filled with original and reworked pyroclastic deposits (Tejedor et al., 2009). These  
172 lithologies are grossly similar in appearance to the later phases of the Tufolitas Laguna del Hunco as  
173 seen inside the caldera, but our geochronologic data presented here indicate that they are not  
174 correlative. The La Barda fauna comes from another incised-valley outcrop ~6 km southwest of  
175 Laguna Fría (Fig. 1). It occurs within tuff units that are interbedded with basalt flows of the Huancache  
176 Formation (Tejedor et al., 2009)

177

## 178 PREVIOUS GEOCHRONOLOGY

179 Several  $^{40}\text{Ar}/^{39}\text{Ar}$  and K-Ar studies have generated age determinations for portions of the  
180 Middle Chubut River Pyroclastic and Volcanic Complex. Archangelsky (1974) used whole-rock K-Ar  
181 methods to determine the age of a single sample of the Ignimbrita Barda Colorada at Cañadón de Loro,  
182 adjacent to Laguna del Hunco (Fig. 1), as  $58.6 \pm 3.0$  Ma ( $\pm 1\sigma$ ; corrected with modern decay constants  
183 using Dalrymple, 1979). Mazzoni et al. (1991) reported twelve whole-rock K-Ar age determinations  
184 from three different labs for lava flows, dikes, and ignimbrites within the complex. Of these, three  
185 samples (VH1, 32-5, 54, and 86-107) appear too young, given reported and observed stratigraphic  
186 relationships, while sample 87-44 appears too old. A possible cause for some of these discrepancies is  
187 low temperature alteration, which was detected in this study using the  $^{40}\text{Ar}/^{39}\text{Ar}$  incremental-heating  
188 technique, but would not have easily been recognizable using older K-Ar methods.

189 At Laguna del Hunco, two paleomagnetic reversals are recorded along with three ca. 52 Ma  
190  $^{40}\text{Ar}/^{39}\text{Ar}$  ages from tuffs recovered from the 170 m local section of the Tufolitas Laguna del Hunco  
191 (Wilf et al., 2003; Wilf et al., 2005a). One of the  $^{40}\text{Ar}/^{39}\text{Ar}$  ages, from the middle of the densely  
192 fossiliferous interval (ash 2211A), was determined from single crystal fusion analyses of sanidine and  
193 is thus considered the most reliable; its age was recalibrated to  $52.22 \pm 0.22$  Ma (Wilf, 2012) relative to  
194 a Fish Canyon standard age of  $28.201 \pm 0.046$  Ma (Kuiper et al., 2008) and a value for  $\lambda^{40}\text{K}$  of  $5.463 \pm$

195  $0.107 \times 10^{-10} \text{ yr}^{-1}$  (Min et al., 2000). The  $52.22 \pm 0.22 \text{ Ma}$  age is widely applied to the rich Laguna del  
196 Hunco fossil assemblage and is not revised here. Finally, the previously mentioned, initial results for  
197 three samples in this study (Gosses, 2006; Gosses et al., 2006) used an age of 28.02 Ma for the Fish  
198 Canyon standard (Renne et al., 1999).

199 The Laguna Fría and La Barda faunas are found above the IBC (Tejedor et al., 2009). The only  
200 previously published lower age constraint for the faunas is the outdated  $^{40}\text{K}$ - $^{40}\text{Ar}$  age determination  
201 discussed above ( $58.6 \pm 3.0 \text{ Ma}$ ) for the caldera-forming IBC (Archangelsky, 1974; Mazzoni et al.,  
202 1991), which is separated from the fossil-bearing outcrops by an erosional unconformity of uncertain  
203 duration. The upper age constraint is the Mazzoni et al. (1991) set of ca. 43 Ma  $^{40}\text{K}$ / $^{40}\text{Ar}$  ages for flows  
204 of the Andesitas Huancache from areas to the west of the fossil exposures; those beds were considered  
205 stratigraphically higher than the La Barda assemblage by Tejedor et al. (2009).

206

207 **METHODS**

208 **Field Localities and Lithofacies**

209 Fossil-bearing lithofacies were examined in thin-section, hand sample, and outcrop in order to  
210 interpret the burial processes and depositional environments associated with fossil preservation.  
211 Observations within the caldera were concentrated at the Laguna del Hunco site, and at three other sites  
212 with lesser plant-fossil preservation (Central Caldera, Escuela Piedra Parada, and Zeballos Oeste; Fig.  
213 1). Our observations also included the Laguna Fría site, which lies outside of the caldera.

214 Four samples from lavas or tuffs were collected and analyzed using the  $^{40}\text{Ar}$ / $^{39}\text{Ar}$  method to  
215 constrain age ranges of several fossil localities within the caldera complex (Table 1). The Ignimbrita  
216 Barda Colorada (Spl. QL-9807) records the principal caldera-forming event (Fig. 2), and it establishes  
217 a maximum age for the initial formation of the fossiliferous caldera-lake deposits of the Tufolitas  
218 Laguna del Hunco (Fig. 1). The lower member of the IBC is calc-alkaline and high in sodium (Aragón

219 et al., 1987), and the upper member is calc-alkaline with a medium to high-K rhyolitic composition  
220 (wt.% SiO<sub>2</sub> = 72-79%; Aragón et al., 1987). The sample dated in this study was collected from the  
221 uppermost IBC at the extra-caldera Laguna Fría locality, where a paleo valley is incised into the IBC  
222 (Fig. 3K; Fig. 4). The IBC at this locality contains multiple cooling units and is at least 100 meters  
223 thick (Mazzoni and Aragón, 1987; Aragón et al., 1987).

224 The Southern Ignimbrite (Spl. IDEPP-04) establishes a minimum age for fossils described from  
225 the underlying, southernmost exposures of the Tufolitas Laguna del Hunco at Piedra Parada (Bippus et  
226 al. 2016, 2019; Bonfleur and Escapa, 2019; Fig. 2). It is a six-meter-thick, red, erosion-resistant  
227 ignimbrite that compromises the uppermost strata in the hills in the far southeastern part of the caldera.  
228 The sample was collected ~2.5 km southeast of Escuela Piedra Parada (Fig. 1). It overlies ash-fall tuffs  
229 and fans of reworked pyroclastic material, and lies stratigraphically several hundred meters above the  
230 gray ashy mudstone facies described at the Escuela Piedra Parada locality.

231 The Laguna Fría Orange Ignimbrite (Spl. VC-20-04) occurs within this locality and establishes  
232 a maximum age for the Laguna Fría fauna (Fig. 2). It is a prominent, fourteen-meter-thick welded  
233 ignimbrite that lies within a paleo-valley eroded into the Upper IBC at the Laguna Fría locality (Fig. 1).  
234 The Orange Ignimbrite thus postdates the IBC, but it predates the Laguna Fría fauna.

235 The Laguna Fría Basalt (Spl. VC-1-04) is an alkali basalt flow of the Andesitas Huancache that  
236 cap the paleo-valley where the Laguna Fría fauna are found (Figs. 1, 2, 3K). It thus establishes a  
237 minimum age for the fauna (Goin et al., 2000, 2001; Tejedor et al., 2005, 2009). At Laguna Fría, the  
238 basalt has an exposed thickness of 40 meters and is one of many basalt flows that interbed and cover  
239 the ignimbrite plateau south and west of this area (Figs. 1, 3L; Aragón et al., 1997; Mazzoni et al.,  
240 1991).

241

## 242 **Geochronology**

243  $^{40}\text{Ar}/^{39}\text{Ar}$  age determinations were made from one alkali basalt (Spl. VC-1-04) and three felsic  
244 ignimbrites (Spl. VC-20-04, IDEPP-04, QL-9807). Groundmass was separated from basalt, and  
245 feldspar (plagioclase and sanidine) crystals were separated from ignimbrites via crushing, sieving to  
246 250–500  $\mu\text{m}$ , magnetic sorting, density separation using methylene iodide, and ultimately hand picking  
247 under a binocular microscope.

248 Sanidine and plagioclase separates were wrapped in aluminum foil, placed in 2.5 cm aluminum  
249 disks, and irradiated along with the 28.201 Ma Fish Canyon sanidine standard (Kuiper et al., 2008) at  
250 the Oregon State University TRIGA reactor in the Cadmium-Lined In-Core Irradiation Tube (CLICIT).  
251 Two mg of plagioclase from sample VC-1-04 were incrementally heated in 24 steps, whereas single  
252 crystal fusion experiments were performed on the other three samples. Incremental heating is the  
253 method of choice when dating basaltic lavas as it permits interrogation of whether alteration or  
254 inheritance have biased the age of the flow (Singer et al., 2019). All experiments were conducted in  
255 the WiscAr laboratory at the University of Wisconsin-Madison using a 50 W CO<sub>2</sub> laser and a Noblesse  
256 multi-collector mass spectrometer following the procedures in Jicha et al. (2016). Weighted mean ages  
257 are calculated with the decay constants of Min et al. (2000) and are reported with analytical  
258 uncertainties at the  $\pm 2\sigma$  analytical uncertainties (95% confidence level). Atmospheric argon value used  
259 is that of Lee et al. (2006).

260

## 261 RESULTS

262 Five different fossil-bearing lithofacies were described for this study. *Laminated mudstone* and  
263 *green tuff* are interpreted to record deposition in a lacustrine basin floor environment. *Gray ashy*  
264 *mudstone* is interpreted to have been deposited both in a lacustrine basin floor environment, and on a  
265 subaerial pyroclastic plain. The *coal lithofacies* is interpreted to record deposition on a vegetated,  
266 waterlogged pyroclastic plain. The *valley-filling pyroclastic lithofacies* is interpreted to record

267 deposition within an incised valley outside of the caldera. An additional fossil-bearing siltstone facies  
268 described in Wilf et al. (2003) was not included during this study.

269

270 *Laminated Mudstone Lithofacies*

271 The laminated mudstone facies occurs only at the Laguna del Hunco locality (Figs. 1, 3A.),,  
272 interbedded with several other lacustrine facies. Beds are several cm to a few dm thick. The laminae  
273 constitute either black and white couplets or black and dark-gray couplets (Fig. 3B), but these two  
274 patterns are not observed within the same bed. Thin-section images show that both the black and the  
275 white laminations contain mud to silt sized crystals and altered glass particles. The black laminations  
276 also have elongate, fibrous, brown organic matter (Fig. 3C). The outcrop surface appears an off-white  
277 or beige color, but a freshly broken surface is medium-brown to black and has a sulfurous odor.  
278 Fractures are either conchoidal or follow laminae. Black fragments of leaves and stems are found  
279 parallel to laminations. Delicate leaf structures are less common.

280 The laminated mudstone facies is interpreted as suspension fall-out of detrital sediment and  
281 organic matter onto a lacustrine basin floor during lulls in volcanic activity, based its grainsize,  
282 preservation fine laminae, organic matter content, and absence of scour, graded beds, or other evidence  
283 for tractive currents (Fig. 4A). The occasionally conchoidal fractures may reflect high silica content.  
284 The laminations could be explained through variability in fine grain sediment influx, organic matter  
285 influx, organic matter preservation, or some combination of these three. Examinations of thin-sections  
286 reveal that the amount of organic material varies between laminations, while the detrital component is  
287 present throughout. This suggests that the laminations may be primarily due to seasonal variation in the  
288 production or preservation of organic material, whereas fine-grained inorganic sediment accumulated  
289 more uniformly through time.

290

291 *Green Tuff Lithofacies*

292        The green tuff facies occurs at the Laguna del Hunco locality (Figure 1), interbedded with the  
293        gray ashy mudstone facies and laminated mudstone facies. This facies consists of pale green, very fine-  
294        to medium-grained tuff with fine- to medium-grained plagioclase and biotite crystals that are often  
295        visible with the naked eye. The tuff has a mottled texture in hand sample but does not display other  
296        sedimentary structure. Fossils in this facies have a light brown stain, but less so than in the gray ashy  
297        mudstone facies. Fossils are generally preserved on planes parallel or at a low angle to bedding. These  
298        fossils typically do not feature as much detail as those in the gray ashy mudstone beds.

299        The green tuff facies is interpreted as an ash-fall tuff deposited in a lacustrine basin-floor  
300        depositional environment, based on its intercalation with laminated mudstone, coarser grainsize, and  
301        lack of sedimentary structures indicative of tractive transport. Accumulation of these types of deposits  
302        typically spans hours to days (Miller and Casadevall, 2000).

303

304        *Gray ashy Mudstone Lithofacies*

305        The gray ashy mudstone facies, found at the Laguna del Hunco, Escuela Piedra Parada, and  
306        Central Caldera localities (Figure 1), has a porcelanitic or cryptocrystalline appearance but lacks  
307        crystals visible with the naked eye or hand lens. It weathers to an off-white color, but is gray to brown  
308        on a fresh break. Beds are typically a few cm to dm in thickness and laterally extensive for hundreds of  
309        meters (Fig. 3D). Thin-sections reveal that 95% of the grains are less than five micrometers (Fig. 3E).  
310        Orange staining is commonly observed on fracture surfaces and fossils, making them more visible.  
311        Fossils occur on planes parallel and sub-parallel to bedding surfaces. Fracture is moderately  
312        conchoidal. Swaley cross-stratification has recently been observed in this facies, suggesting episodes of  
313        high-energy wave and combined-flow events in a lake (J.M. Krause and E.A. Hajek, pers. comm.,  
314        2019).

315        At the Laguna del Hunco locality this facies contains well-preserved fossil plants, frogs, fish,  
316        and insects. Many whole leaves are preserved (Fig. 3F) with well-preserved venation and insect

317 damage, along with delicate flowers, fruits, and insect body-fossils, as reported extensively elsewhere  
318 (see Introduction). Bed geometries include sheets, lenses, lobes, and drapes. Gray ashy mudstone beds  
319 at the Laguna del Hunco locality are typically intercalated with turbidite, debris-flow, green tuff,  
320 laminated mudstone, and green-brown mudstone beds (Figs. 3D, G). The sediment gravity-flow  
321 deposits exhibit flame structures and meter-scale soft-sediment folds, which together with current  
322 ripples indicate a depositional gradient that sloped toward the east or northeast, away from the  
323 resurgent caldera dome (see Fig. 1).

324 Orange staining and fossils are less common at the Escuela Piedra Parada and Central Caldera  
325 localities (Fig. 1). In contrast to the Laguna del Hunco locality, the gray ashy mudstone beds are  
326 frequently stacked on top one another with few interbedded strata, and are associated with extrusive  
327 glass domes (Fig. 3H). The only interbedded units are volcaniclastic sandstone beds rich in angular to  
328 subangular crystals and tuff clasts. However, the sections above and below the gray ashy mudstone  
329 intervals do contain debris-flows, ash-fall tuffs, ash-flow tuffs, and double-graded pyroclastic debris-  
330 flows. Five silicified tree trunks up to 11 m long were observed within the ash flow tuffs at Escuela  
331 Piedra Parada (Fig. 3I), in the same general area that preserved a permineralized fossil fern trunk  
332 (Bomfleur and Escapa, 2019; Figure 1, localities 3 and 5). In two cases, the tree roots are preserved in  
333 life orientation, whereas the trunks are oriented sub-parallel to bedding and aligned parallel.

334 This facies is interpreted to have been deposited in two different environments. At the Laguna  
335 del Hunco locality, it is interbedded with turbidites and other facies indicating a lacustrine basin-floor  
336 depositional environment (Fig. 4A). The presence of swaley cross stratification in the gray ashy  
337 mudstone implies at least partial reworking by waves, possibly in combination with unidirectional flow  
338 (cf., Dumas and Arnott, 2006). At the Central Caldera and Escuela Piedra Parada localities, it was  
339 deposited on a subaerial pyroclastic plain. Associated ash flows knocked down trees and covered the  
340 ground surface. Sheet flood transport processes, shallow channelization, and air-fall pyroclastic events  
341 deposited centimeter to decimeter beds of varying geometries and levels of immaturity (Fig. 4B).

342 Meter-scale welded ignimbrites filled-in and reorganized topography above and below the strata  
343 containing gray ashy mudstone facies.

344

345 *Coal Lithofacies*

346 The coal facies occurs at the Zeballos Oeste (Fig. 1). A single cm-thick coal seam is observed in  
347 place, and is encased by brown-gray tuff. Fragmented plant material is preserved on distorted, sub-  
348 parallel surfaces, but leaves are less well preserved than in other facies. Directly below the coal seam  
349 are dm-scale, compensationally-stacked beds with a lenticular geometry. The coal is overlain by a  
350 massive, several-meter-thick bed that contains coaly intraclasts.

351 The coal facies is interpreted as a leaf mat deposited under reducing conditions on a vegetated,  
352 waterlogged pyroclastic lake margin (Fig. 4C). Coal intraclasts in the overlying beds suggest erosion  
353 of up-dip coal forming environments.

354

355 *Valley-Filling Pyroclastic Lithofacies*

356 The valley-filling pyroclastic facies examined for this study is confined to a northwest-  
357 southeast-oriented paleo valley incised into the Ignimbrita Barda Colorado southeast of the caldera (the  
358 Laguna Fría locality; Figs. 1, 2). A modern valley that is oriented northeast-southwest exposes multiple  
359 paleo-valleys in this area. The valley-filling pyroclastic facies is broadly defined to include non-welded  
360 tuffaceous deposits and reworked pyroclastic deposits (Fig. 3J). Dm-thick beds can have erosive bases,  
361 are generally matrix-supported and fining-upwards, and contain lapilli. In contrast, cm-thick beds are  
362 more likely to be grain-supported and contain crossbedding and root casts. Some of these beds are  
363 dominated by crystal grains or ash lapilli of multiple compositions, with a marked reduction in fine-  
364 grained matrix. A few beds have sub-angular tuff clasts up to 1 cm. Most beds continue across the  
365 entire outcrop. A small number of the grain-supported beds have very broad U-shaped geometries up to  
366 two meters across. This facies contains abundant vertebrate specimens described as the Laguna Fría

367 fauna (Tejedor et al., 2005; 2009). Silicified trunk material was also found as float at this locality, but  
368 no leaves or other plant compressions were found. The Laguna Fría vertebrate assemblage occurs  
369 predominantly above the prominent Laguna Fría Orange Ignimbrite and below the Laguna Fría  
370 Capping Basalt (Fig. 3K).

371 The valley-filling pyroclastic facies is interpreted as a combination of primary and reworked  
372 pyroclastic deposits within an extra-caldera paleo-valley incised into the Ignimbrita Barda Colorada  
373 (Fig. 4D). Composition, grain distribution, and fluid escape tubes suggest some of the pyroclastic  
374 material was deposited by ash-fall and other ash-cloud mechanisms. Some beds were buried intact by  
375 later pyroclastic eruptions. Others were partially or fully reworked by a combination of fluvial and  
376 sheet flood processes. This is especially apparent in the tops of some dm-scale pyroclastic beds where  
377 centimeter-scale cross-bedded intervals, ripples, and well-sorted volcaniclastic sands suggest partial  
378 reworking of the tops of the beds only. Channels of only a few meters width were observed, suggesting  
379 an environment controlled by small-scale fluvial and sheet-flood processes. The depositional  
380 environment was akin to a partially filled alluvial canyon.

381

382  **$^{40}\text{Ar}/^{39}\text{Ar}$  Ages**

383 *The Upper Ignimbrita Barda Colorada*

384 Laser fusion experiments were performed on 16 individual crystals. Of these, only two yield  
385 K/Ca ratios consistent with sanidine, whereas the remainder were plagioclase and thus were excluded  
386 from analysis. The weighted mean age of the two sanidine dates is  $52.54 \pm 0.17$  Ma (Fig. 5).

387

388 *Southern Ignimbrite*

389 Plagioclase was separated from this ignimbrite because no sanidine was present. Eighteen laser  
390 fusion experiments on individual plagioclase crystals give a weighted mean age of  $49.38 \pm 0.12$  Ma  
391 (Fig. 5). However, the isochron calculated from these 18 crystals gives an intercept of  $310.7 \pm 3.7$ ,

392 which is significantly higher than the atmospheric value. Hence, the isochron age of  $49.19 \pm 0.24$  Ma is  
393 preferred.

394

395 *Laguna Fría Orange Ignimbrite*

396 Plagioclase crystals were separated from this ignimbrite because no sanidine was present.

397 Single-crystal laser fusion experiments were performed on 19 plagioclase crystals. Eleven of these  
398 experiments produced radiogenic  $^{40}\text{Ar}^*$  concentrations lower than 70%, which may represent post-  
399 depositional loss of  $^{40}\text{Ar}^*$ . Excluding these from the results yields a distribution of dates with a  
400 weighted mean age of  $49.00 \pm 0.16$  Ma (Fig. 5). However, the isochron calculated from these 19  
401 crystals gives an intercept of  $290.5 \pm 3.3$ , which is lower than the atmospheric value. Hence, the  
402 isochron age of  $49.26 \pm 0.30$  Ma is preferred.

403

404 *Laguna Fría Capping Basalt*

405 A 24-step incremental heating experiment on a two mg groundmass separate yields an age  
406 spectrum with low temperature steps characterized by younger apparent ages. We interpret this  
407 discordance to reflect argon loss due to weathering and excluded the younger steps in the calculation of  
408 a plateau age. Notwithstanding, an age plateau, defined by 87% of the  $^{39}\text{Ar}$  released, signifies that the  
409 basalt has a largely homogenous distribution of radiogenic argon, and yields an apparent age of  $43.50 \pm$   
410  $1.14$  Ma, which is indistinguishable from the inverse isochron age of  $43.50 \pm 2.22$  Ma (Fig. 6).

411

## 412 **DISCUSSION**

413 The  $^{40}\text{Ar}/^{39}\text{Ar}$  ages reported here represent new, fully-documented constraints on the timing of  
414 the Laguna del Hunco flora and Laguna Fría fauna (Figure 7). The age of the Ignimbrita Barda  
415 Colorado was previously reported as  $58.6 \pm 3.0$  Ma ( $\pm 1\sigma$ ) based on older  $^{40}\text{K}/^{40}\text{Ar}$  techniques  
416 (Archangelsky, 1974), but can now be revised to  $52.54 \pm 0.17$  Ma ( $\pm 2\sigma$ ), a difference of ~6 million

417 years. The new age is not distinguishable from the  $^{40}\text{Ar}/^{39}\text{Ar}$  ages of tuffs at the Laguna del Hunco  
418 locality ( $52.22 \pm 0.22$  Ma; Wilf, 2012) given the  $2\sigma$  uncertainties, a finding that is consistent with rapid  
419 initial deposition (Fig. 2 and Fig. 7) following the formation of a topographic depression during or  
420 shortly after the initial caldera eruption.

421 The southern ignimbrite occurs hundreds of meters stratigraphically above the gray ashy  
422 mudstone facies at Escuela Piedra Parada. It's  $49.19 \pm 0.24$  Ma age therefore establishes a minimum  
423 age for the gray ashy mudstone facies at this locality. The same constraint may also extend to the gray  
424 ashy mudstone facies at the Laguna del Hunco locality, if deposition of this facies in both areas  
425 occurred in response to a common eruptive history. The southern ignimbrite may also constrain the  
426 age of fossil fern trunks located  $\sim 5$  km to the west (Bippus et al., 2019; Bomfleur and Escapa, 2019;  
427 Fig. 1).

428 Maximum and minimum age constraints for the Laguna Fría fauna are defined by the  
429 underlying  $49.26 \pm 0.30$  Ma Laguna Fría Orange Ignimbrite, and the overlying  $43.50 \pm 1.14$  Ma  
430 Laguna Fría capping basalt. The relationship of these ages to the nearby La Barda fauna remains  
431 unclear however. Tejedor et al. (2009) inferred that the Laguna Fría capping basalt represents a basal  
432 basalt flow of the Andesitas Huancache, and that the La Barda fauna lies stratigraphically above this  
433 basal flow and therefore must be younger. They assumed a 47-45 Ma age range for the La Barda  
434 fauna, based on a preliminary  $^{40}\text{Ar}/^{39}\text{Ar}$  age determination for the Laguna Fría basalt of  $47.89 \pm 1.21$  Ma  
435 (Gosses et al., 2006) and on  $^{40}\text{K}/^{40}\text{Ar}$  ages of  $\sim 43$  Ma for an overlying lava flow (Mazzoni et al., 1991).  
436 If the stratigraphic relationships inferred by Tejedor et al. (2009) are correct, our revised age for the  
437 Laguna Fría capping basalt requires that the La Barda fauna is in fact younger than  $\sim 43.50$  Ma. It must  
438 be noted however that these localities lie  $\sim 6$  km apart in an area that experienced a spatially complex  
439 history of basaltic eruptions. The detailed stratigraphy of these flows has not been mapped, making  
440 precise correlation between sites problematic. Examination of satellite imagery (Fig. 3L) suggests  
441 that both localities lie stratigraphically below a prominent mesa-forming basalt, which approximately

442 corresponds to the Laguna Fría capping basalt sampled in this study. Tejedor et al. (2009) reported  
443 faunistic similarities between the two fossil assemblages. Based on the data presented here, we cannot  
444 conclusively determine the age relationship between the La Barda and Laguna Fría fauna; it appears  
445 possible that they are the same age. A more detailed investigation of field relationships and basalt ages  
446 is needed to resolve this ambiguity. More broadly, the available age constraints on these faunas overlap  
447 with the age ranges proposed by Krause et al. (2017) for the Riochican and Vacan fauna, and therefore  
448 do not directly support the existence of a temporally distinct “Sapoan” SALMA.

449 Tejedor et al. (2009) considered the vegetation and paleoclimate for the Laguna Fría and La  
450 Barda mammals to be best represented by the ca. 52.2 Ma Laguna del Hunco and ca. 47.7 Ma Río  
451 Pichileufú (Río Negro) rainforest floras (Berry, 1938; Wilf et al., 2005a; Wilf, 2012). These sites show  
452 that generally similar floral composition, elevated floral richness, and a mesic rainforest environment  
453 persisted in the region for an extended period of time that encompassed these faunas. Our new  
454 geochronologic results show that this argument remains plausible, but only in the older part of its  
455 possible age range. The younger end of the permissible age range, extending to  $43.50 \pm 1.14$  Ma,  
456 corresponds with substantially cooler and drier conditions and major vegetation changes, both  
457 regionally and globally (Palazzi and Barreda, 2007; Zachos et al., 2008; Dunn et al., 2015)

458

## 459 CONCLUSIONS

460 The Middle Chubut River Pyroclastic and Volcanic Complex preserves fossil assemblages  
461 associated with multiple terrestrial, volcaniclastic lithofacies, that lie stratigraphically above the  
462 caldera-forming Ignimbrita Barda Colorada. A new  $^{40}\text{Ar}/^{39}\text{Ar}$  age for the caldera-forming Ignimbrita  
463 Barda Colorada of  $52.54 \pm 0.17$  Ma is preferred over previous age determinations. This age is  
464 indistinguishable, given the  $2\sigma$  uncertainties, from a  $52.22 \pm 0.22$  Ma  $^{40}\text{Ar}/^{39}\text{Ar}$  age previously reported  
465 for a tuff at the Laguna del Hunco fossil locality (Wilf, 2012), demonstrating rapid onset of lacustrine  
466 deposition and prolific fossil preservation following caldera subsidence. An ignimbrite deposited above

467 the fossil-strata gives an age of  $49.19 \pm 0.24$  Ma, collectively indicating that the Laguna del Hunco  
468 flora broadly coincided with the Early Eocene Climatic Optimum (~53-50 Ma; Zachos et al., 2008).

469 The Laguna Fría fauna is younger, constrained between the  $49.26 \pm 0.30$  Ma Laguna Fría  
470 orange ignimbrite and the  $43.50 \pm 1.14$  Ma Laguna Fría capping basalt. The age of the nearby La  
471 Barda fauna is more difficult to confidently determine. If previous stratigraphic relations inferred by  
472 Tejedor et al. (2009) are correct, then the La Barda fauna is at least 2 million years younger than its  
473 previously assumed age range of 47-45 Ma. The detailed stratigraphy of basaltic eruptions is poorly  
474 known however, and it is therefore possible that the La Barda and Laguna Fría faunas are similar in  
475 age. Finally, the Laguna Fría age range overlaps with the age ranges proposed by Krause et al. (2017)  
476 for the Riochican and Vacan faunas and therefore does not directly support the existence of a  
477 temporally distinct “Sapoan” SALMA.

478

## 479 **ACKNOWLEDGMENTS**

480 We thank Jessica Lopez for help in the field, Lauren Chetel and Bryan Wathen for assistance in  
481 the laboratory, and E.A. Hajek and J.M. Krause for their helpful comments on an earlier version of the  
482 manuscript. We also thank two anonymous reviewers for their constructive comments. This research  
483 was supported by a 2005 AAPG Student Grant-In-Aid, NSF grants DEB-0345750, DEB-1556666, and  
484 EAR-1925755, and the University of Wisconsin Department of Geoscience.

485

## 486 **REFERENCES**

487  
488 Alric, V., 1997, Estudio de los basaltos portadores de xenolitos ultrabásicos aflorantes en la Hoja 45c,  
489 Paso de Indios, Provincia del Chubut [Ph.D. thesis]: San Juan Bosco, Universidad Nacional de  
490 la Patagonia, 168 p.  
491 Ameghino, F., 1906, Les formations sédimentaires du Crétacé Supérieur et du Tertiaire de Patagonie  
492 avec un parallèle entre leurs faunes mammalogiques et celles de l'ancien continent: Anales del  
493 Museo Nacional de Historia Natural de Buenos Aires, v. 15, no. 8, p. 1-568.  
494 Aragón, E., Aguilera, Y. D., González, P. D., Gómez Peral, L., Cavarozzi, C. E., and Ribot, A., 2001,  
495 El Intrusivo Florentina del complejo volcánico piroclástico del Río Chubut medio (Paleocene-

496 Eoceno medio): un ejemplo de etmolito o embudo: Revista de la Asociación Geológica  
497 Argentina, v. 56, no. 2, p. 161-172.

498 Aragón, E., and Mazzoni, M.M., 1997, Geología y estratigrafía del complejo volcánico piroclástico del  
499 Río Chubut medio (Eoceno), Chubut, Argentina: Revista de la Asociación Geológica Argentina,  
500 v. 52, no. 3, p. 243-256.

501 Aragón, E., and Romero, E. J., 1984, Geología, paleoambientes y paleobotánica de yacimientos  
502 Terciarios del occidente de Río Negro, Neuquén y Chubut: Actas del IX Congreso Geológico  
503 Argentino, San Carlos de Bariloche, v. 4, p. 475-507.

504 Aragón, E., Castro, A., Diaz-Alvarado, J., Pinotti, L., D'eramo, F., Demartis, M., Coniglio, J.,  
505 Hernando, I., and Rodriguez, C., 2018, Mantle derived crystal-poor rhyolitic ignimbrites:  
506 Eruptive mechanism from geochemical and geochronological data of the Piedra Parada caldera,  
507 Southern Argentina: Geoscience Frontiers, v. 9, no. 5, p. 1529-1553.

508 Aragón, E., González, P. D., Aguilera, Y., Marquett, C., Cavarozzi, C., and Ribot, A., 2004, El domo  
509 vitrofírico Escuela Piedra Parada Piedra Parada del Complejo Volcanico Piroclastico del Río  
510 Chubut Medio: Revista de la Asociación Geológica Argentina, v. 59, no. 4, p. 634-642.

511 Aragón, E., Mazzoni, M.M., and Merodio, J., 1987, Caracterización geoquímica de Ignimbrita Barda  
512 Colorada en el Río Chubut medio, Argentina; Actas 10º Congreso Geológico Argentino, p. 171-  
513 173.

514 Archangelsky, S., 1974, 2005, La paleobotánica en Argentina y su desarrollo durante los últimos 50  
515 años: Asociación Paleontológica Argentina. Publicación Especial, v. 10, p. 37-49.

516 Archangelsky, S., 1974, Sobre la edad de la taflora de la Laguna del Hunco, Prov. de Chubut:  
517 Ameghiniana, v. 11, p. 413- 417.

518 Azpelicueta, M. M., and Cione, A. L., 2011, Re-description of the Eocene catfish *Bachmannia*  
519 *chubutensis* (Teleostei: Bachmanniidae) of southern South America: Journal of Vertebrate  
520 Paleontology, v. 31, p. 258-269.

521 Báez, A. M., and Pugener, L. A., 2003, Ontogeny of a new Palaeogene pipid frog from southern South  
522 America and xenopodinomorph evolution: Zoological Journal of the Linnean Society, v. 139,  
523 no. 3, p. 439-476.

524 Báez, A. M., and Trueb, L., 1997, Redescription of the Paleogene *Shelania pascuali* from Patagonia  
525 and its bearing on the relationships of fossil and Recent pipoid frogs: Scientific Papers, Natural  
526 History Museum, The University of Kansas, v. 4, p. 1-41.

527 Barreda, V. D., Palazzesi, L., Tellería, M. C., Katinas, L., Crisci, J. V., Bremer, K., Passalia, M. G.,  
528 Corsolini, R., Rodríguez Brizuela, R., and Bechis, F., 2010, Eocene Patagonia fossils of the  
529 daisy family: Science, v. 329, no. 5999, p. 1621.

530 Bellosi, E. S., 2010, Physical stratigraphy of the Sarmiento Formation (middle Eocene-lower Miocene)  
531 at Gran Barranca, central Patagonia, in Madden, R. H., Carlini, A. A., Vucetich, M. G., and  
532 Kay, R. F., eds., The Paleontology of Gran Barranca: Cambridge, UK, Cambridge University  
533 Press, p. 19-31.

534 Berry, E. W., 1925, A Miocene flora from Patagonia: Johns Hopkins University Studies in Geology, v.  
535 6, p. 183-251.

536 Berry, E. W., 1938, Tertiary flora from the Río Pichileufú, Argentina: Geological Society of America  
537 Special Paper, v. 12, p. 1-149.

538 Bippus, A. C., Escapa, I. H., and Tomescu, A., 2016, Tiny ecosystems: bryophytes and other biotic  
539 interactions around an osmundaceous fern from the Eocene of Patagonia: Botany 2016,  
540 Savannah Georgia, Abstract 243.

541 Bippus, A. C., Escapa, I. H., Wilf, P., and Tomescu, A. M. F., 2019, Fossil fern rhizomes as a model  
542 system for exploring epiphyte community structure across geologic time: evidence from  
543 Patagonia: PeerJ, v. 7, p. e8244.

544 Bomfleur, B., and Escapa, I., 2019, A silicified Todea trunk (Osmundaceae) from the Eocene of  
545 Patagonia: *Paläontologische Zeitschrift*, doi:10.1007/s12542-019-00479-6.

546 Busby-Spera, C., 1984, Large-volume rhyolite ash flow eruptions and submarine caldera collapse in the  
547 lower Mesozoic Sierra Nevada, California: *Journal of Geophysical Research B*, v. 89, p. 8417-  
548 8427.

549 Carlini, A.A., Ciancio, M., and Scillato-Yane', G.J., 2005, Los xenarthros de Gran Barranca: más de 20  
550 Ma de Historia in *Actas 16º Congreso Geológico Argentino*, La Plata, p. 315-322.

551 Casamiquela, R. M., 1961, Un pipoideo fósil de Patagonia: *Revista del Museo de La Plata, Sección*  
552 *Paleontología*, v. 4, no. 22, p. 71-123.

553 Clyde, W. C., Wilf, P., Iglesias, A., Slingerland, R. L., Barnum, T., Bijl, P. K., Bralower, T. J.,  
554 Brinkhuis, H., Comer, E. E., Huber, B. T., Ibañez-Mejia, M., Jicha, B. R., Krause, J. M.,  
555 Schueth, J. D., Singer, B. S., Raigemborn, M. S., Schmitz, M. D., Sluijs, A., and Zamaloa, M.  
556 C., 2014, New age constraints for the Salamanca Formation and lower Río Chico Group in the  
557 western San Jorge Basin, Patagonia, Argentina: *Geological Society of America Bulletin*, v. 126,  
558 no. 2-4, p. 289-306.

559 Comer, E. E., Slingerland, R. L., Krause, J. M., Iglesias, A., Clyde, W. C., Raigemborn, M. S., and  
560 Wilf, P., 2015, Sedimentary facies and depositional environments of diverse early Paleocene  
561 floras, north-central San Jorge Basin, Patagonia, Argentina: *Palaios*, v. 30, p. 553-573.

562 Dalla Salda, L.H., and Franzese, J., 1987, Las Megaestructuras de macizo y cordillera Norpatagónica  
563 Argentina y la génesis de las cuencas volcano-sedimentarias terciarias: *Revista Geológica de*  
564 *Chile*, v. 31, p. 3-13.

565 Dalrymple, G., 1979, Critical tables for conversion of K-Ar ages from old to new constraints: *Geology*,  
566 v. 7, p. 558-560.

567 Diessel, C.F.K., 1992, Coal-Bearing Depositional Systems: New York City, Springer-Verlag Telos.  
568 721 p.

569 Dolgopol de Sáez, M., 1941, Noticias sobre peces fósiles Argentinos. Siluroideos Terciarios de Chubut:  
570 Notas del Museo de La Plata, v. 35, p. 451-457.

571 Dumas, S., and Arnott, R.W.C., 2006, Origin of hummocky and swaley cross-stratification-the  
572 controlling influence of unidirectional current strength and aggradation rate: *Geology*, v. 34, p.  
573 1073-1076.

574 Dunn, R. E., Madden, R. H., Kohn, M. J., Schmitz, M. D., Strömberg, C. A. E., Carlini, A. A., Ré, G.  
575 H., and Crowley, J., 2013, A new chronology for middle Eocene-early Miocene South  
576 American Land Mammal Ages: *Geological Society of America Bulletin*, v. 125, no. 3-4, p. 539-  
577 555.

578 Dunn, R. E., Strömberg, C. A. E., Madden, R. H., Kohn, M. J., and Carlini, A. A., 2015, Linked  
579 canopy, climate, and faunal change in the Cenozoic of Patagonia: *Science*, v. 347, no. 6219, p.  
580 258-261.

581 Feruglio, E., 1949, Descripción geológica de la Patagonia, vol. II, Buenos Aires, Ministerio de  
582 Industria y Comercio de la Nación, Dirección General de Yacimientos Petrolíferos Fiscales.

583 Fidalgo, P., and Smith, D. R., 1987, A fossil Siricidae (Hymenoptera) from Argentina: *Entomological*  
584 *News*, v. 98, no. 2, p. 63-66.

585 Flynn, J. J., and Swisher, C. C., III, 1995, Cenozoic South American Land Mammal Ages: correlation  
586 to global geochronologies, Volume *Geochronology time scales and global stratigraphic*  
587 *correlation*, SEPM, p. 317-333.

588 Frenguelli, J., 1943, Restos de Casuarina en el Mioceno de El Mirador, Patagonia central: *Notas del*  
589 *Museo de La Plata*, v. 8, no. 56, p. 349-354.

590 Gandolfo, M. A., Hermsen, E. J., Zamaloa, M. C., Nixon, K. C., González, C. C., Wilf, P., Cúneo, N.  
591 R., and Johnson, K. R., 2011, Oldest known *Eucalyptus* macrofossils are from South America:  
592 *PLoS One*, v. 6, no. 6, p. e21084.

593 Gaudry, M. A., 1906, Fossiles de Patagonie. Étude sur une portion du monde antarctique: Annales de  
594 Paléontologie, v. 1, p. 101-143.

595 Gelfo, J. N., Goin, F. J., Woodburne, M. O., and de Muizon, C., 2009, Biochronological relationships  
596 of the earliest South American Paleogene mammalian faunas: *Palaeontology*, v. 52, no. 1, p.  
597 251-269.

598 Goin, F. J., Case, J. A., Woodburne, M. O., Vizcaíno, S. F., and Reguero, M. A., 1999, New  
599 discoveries of "opossum-like" marsupials from Antarctica (Seymour Island, medial Eocene):  
600 *Journal of Mammalian Evolution*, v. 6, no. 4, p. 335-365.

601 Goin, F. J., Gelfo, J. N., Chornogubsky, L., Woodburne, M. O., and Martin, T., 2012a, Origins,  
602 radiations, and distribution of South American mammals: from greenhouse to icehouse worlds,  
603 in Patterson, B. D., and Costa, L. P., eds., *Bones, Clones, and Biomes: the History and*  
604 *Geography of Recent Neotropical Mammals*: Chicago, University of Chicago Press, p. 20-50.

605 Goin, F. J., Tejedor, M., Chornogubsky, L., López, G. M., Gelfo, J. N., Bond, M., Woodburne, M. O.,  
606 Gurovich, Y., and Reguero, M., 2012b, Persistence of a Mesozoic, non-therian mammalian  
607 lineage (Gondwanatheria) in the mid-Paleogene of Patagonia: *Naturwissenschaften*, v. 99, no. 6,  
608 p. 449-463.

609 Goin, F. J., Vieytes, E. C., Gelfo, J. N., Chornogubsky, L., Zemicz, A. N., and Reguero, M. A., 2018,  
610 New metatherian mammal from the early Eocene of Antarctica: *Journal of Mammalian*  
611 *Evolution*, doi: 10.1007/s10914-10018-19449-10916.

612 Goin, F., Tejedor, B. M., Lopez, G., and Reguero, M., 2000, Mamíferos Eocenos de Paso del Sapo,  
613 Chubut, Argentina: *Ameghiniana*, v. 37, p. 25R-26R.

614 Goin, F., Tejedor, M., and Abello, A., 2001, Conclusiones preliminares sobre la asociación de  
615 marsupiales Paleogenos de Laguna Giordanella, Paso del Sapo, Chubut, Argentina; Eocene  
616 Medio: *Ameghiniana*, v. 38, p. 9R-10R.

617 Gosses, J., 2006, Stratigraphy and 40Ar/39Ar geochronology of the Laguna del Hunco Formation: a  
618 lacustrine and sub-aerial caldera moat formation [M.S.: University of Wisconsin, Madison, 1-  
619 265 p.

620 Gosses, J., Carroll, A., Aragón, E., and Singer, B., 2006, The Laguna del Hunco formation: Lacustrine  
621 and Sub-Aerial Caldera Fill, Chubut Province, Argentina: *Geological Society of America*  
622 *Annual Meeting Abstracts*, v. 38, no. 7, p. 502.

623 Harding, I. C. and Chant, L.S., 2000, Self-sedimentation diatom mats as agents of exceptional fossil  
624 preservation in the Oligocene Florissant Lake Beds, Colorado, United States: *Geology*, v. 29,  
625 no. 3, p. 195-198.

626 Iannelli, S. B., Litvak, V. D., Fernández Paz, L., Folguera, A., Ramos, M. E., and Ramos, V. A., 2017,  
627 Evolution of Eocene to Oligocene arc-related volcanism in the North Patagonian Andes (39–  
628 41°S), prior to the break-up of the Farallon plate: *Tectonophysics*, v. 696–697, p. 70-87.

629 Ivany, L.C. 2007, Contributions to the Eocene climatic record of the Antarctic Peninsula: United States  
630 Geological Survey Open File Report 1047, U.S. Geological Survey and the National Academies  
631 Extended Abstracts, v. 68, p. 1-4.

632 Jicha, B.R., Singer, B.S., Sobol, P., 2016. Re-evaluation of the ages of 40Ar/39Ar sanidine standards  
633 and supereruptions in the western U.S. using a Noblesse multi-collector mass spectrometer.  
634 *Chem. Geol.* 431, 54–66, <https://doi.org/10.1016/j.chemgeo.2016.03.024>.

635 Kay, R.F., Madden, R.H., Vucetich, M.G., Carlini, A.G., Mazzoni, M.M., Re, G., Heizler, M., and  
636 Sandeman, H., 1999, Revised geochronology of the Casamayoran South American Land  
637 Mammal Age: climatic and biotic implications: *Proceedings of the National Academy of*  
638 *Sciences of the United States of America*, v. 95, p. 13235–13240.

639 Kooyman, R. M., Wilf, P., Barreda, V. D., Carpenter, R. J., Jordan, G. J., Sniderman, J. M. K., Allen,  
640 A., Brodribb, T. J., Crayn, D., Feild, T. S., Laffan, S. W., Lusk, C. H., Rossetto, M., and  
641 Weston, P. H., 2014, Paleo-Antarctic rainforest into the modern Old World Tropics: the rich

642 past and threatened future of the "southern wet forest survivors": American Journal of Botany,  
643 v. 101, no. 12, p. 2121-2135.

644 Krause, J. M., Clyde, W. C., Ibañez-Mejía, M., Schmitz, M., Barnum, T., Bellosi, E., and Wilf, P.,  
645 2017, New age constraints for early Paleogene strata of central Patagonia, Argentina:  
646 implications for the timing of South America land mammal ages: Geological Society of  
647 America Bulletin, v. doi: 10.1130/B31561.1.

648 Kuiper, K. F., Deino, A., Hilgen, F.J., Krijgsman, W., Renne, P.R., and Wijbrans, J.R., 2008,  
649 Synchronizing Rock Clocks of Earth History: Science, v. 320, p. 500-504.

650 Labandeira, C. C., Wilf, P., Cuneo, N. R., and Johnson, K., 2004, Eocene plant-insect associational  
651 diversity at Laguna del Hunco, Patagonia, Argentina: Geological Society of America, Abstracts  
652 with Programs, v. 36, no. 5, p. 95.

653 Lawver, L. A., Gahagan, L. M., and Dalziel, I. W. D., 2011, A different look at gateways: Drake  
654 Passage and Australia/Antarctica, in Anderson, J. B., and Wellner, J. S., eds., Tectonic,  
655 climatic, and cryospheric evolution of the Antarctic Peninsula: Washington, DC, AGU, p. 5-33.

656 Lee, J.-Y., Martí, K., Severinghaus, J.P., Kawamura, K., Yoo, H.-S., Lee, J.B., Kim, J.S., 2006. A  
657 redetermination of the isotopic abundance of atmospheric Ar. *Geochim. Cosmochim. Acta* 70,  
658 4507–4512.

659 Lipman, P.W., 1997, Subsidence of ash-flow calderas: relation to caldera size and magma-chamber  
660 geometry: *Bulletin of Volcanology*, v. 59, p. 198-218.

661 Lorente, M., 2016, Isolated litopterna postcranial remains from La Barda Tuff (early Eocene), Paso del  
662 Sapo, Chubut, Argentina: proposed association with dental taxa and their implications:  
663 *Ameghiniana*, v. 53, no. 1, p. 26-38.

664 Lorente, M., Chornogubsky, L., and Goin, F. J., 2016, On the existence of non-microbiotherian  
665 Australidelphian marsupials (Diprotodontia) in the Eocene of Patagonia: *Palaeontology*, v. 59,  
666 no. 4, p. 533-547.

667 Lorente, M., Chornogubsky, L., and Goin, F. J., 2016, On the existence of non-microbiotherian  
668 Australidelphian marsupials (Diprotodontia) in the Eocene of Patagonia: *Palaeontology*, v. 59,  
669 no. 4, p. 533-547.

670 Madden, R.H., Bellosi, E., Carlini, A.A., Heizler, M., Vilas, J.J., Re, G., Kay, R.F., and Vucetich,  
671 M.G., 2005, Geochronology of the Sarmiento Formation at Gran Barranca and elsewhere in  
672 Patagonia: calibrating middle Cenozoic mammal evolution in South America: *Actas 16º*  
673 Congreso Geológico Argentino, La Plata, no. 4, p. 411-412.

674 Mazzoni, M. M., Aragón, E., and Merodio, J. C., 1989, La Ignimbrita Barda Colorada del complejo  
675 volcánico piroclástico del Río Chubut Medio: *Revista de la Asociación Geológica Argentina*, v.  
676 44, no. 1-4, p. 246-258.

677 Mazzoni, M. M., Kawashita, K., Harrison, S., and Aragón, E., 1991, Edades radimétricas Eocenas.  
678 Borde occidental del Macizo Norpatagónico: *Revista de la Asociación Geológica Argentina*, v.  
679 46, no. 1-2, p. 150-158.

680 Mazzoni, M. M., Kawashita, K., Harrison, S., and Aragón, E., 1991, Edades radimétricas Eocenas.  
681 Borde occidental del Macizo Norpatagónico: *Revista de la Asociación Geológica Argentina*, v.  
682 46, no. 1-2, p. 150-158.

683 Mazzoni, M.M., and Aragón, E., 1987, La Ignimbrita Barda Colorada del Complejo Volcánico  
684 Piroclástico del Río Chubut Medio: *Actas 10º Congreso Geológico Argentino*, La Plata, p. 168-  
685 170.

686 Melendi, D. L., Scafati, L. H., and Volkheimer, W., 2003, Palynostratigraphy of the Paleogene Huitrera  
687 Formation in N-W Patagonia, Argentina: *Neues Jahrbuch für Geologie und Paläontologie-*  
688 *Abhandlungen*, v. 228, no. 2, p. 205-273.

689 Min, K., Mundil, R., Renne, P.R., Ludwig, K.R., 2000. A test for systematic errors in  $40\text{Ar}/39\text{Ar}$   
690 geochronology through comparison with U/Pb analysis of a 1.1-Ga rhyolite. *Geochim.*  
691 *Cosmochim. Acta* 64, 73–98.

692 Palazzi, L., and Barreda, V., 2007, Major vegetation trends in the Tertiary of Patagonia (Argentina):  
693 a qualitative paleoclimatic approach based on palynological evidence: *Flora*, v. 202, p. 328-337.

694 Pascual, R., 2006, Evolution and geography: the biogeographic history of South American land  
695 mammals: *Annals of the Missouri Botanical Garden*, v. 93, no. 2, p. 209-230.

696 Pascual, R., and Ortíz-Jaureguizar, E., 1991, El ciclo faunístico Cochabambiano (Paleoceno temprano):  
697 su incidencia en la historia biogeográfica de los mamíferos sudamericanos in Suárez Soruco, R.,  
698 ed., *Fósiles y facies de Bolivia: Vertebrados*, v. 1, *Revista Técnica de Yacimientos Petrolíferos*  
699 *Fiscales Bolivianos*, v. 12, no. 3-4, p. 559–574.

700 Pascual, R., Archer, M., Ortiz-Jaureguizar, E., Prado, J. L., Godthelp, H., and Hand, S. J., 1992, First  
701 discovery of monotremes in South America: *Nature*, v. 356, no. 6371, p. 704-706.

702 Petersen, C. S., 1946, Estudios geológicos en la región del Río Chubut medio: *Boletín de la Dirección*  
703 *Nacional de Geología y Minería*, no. 59, 137 p.

704 Petrulevičius, J., 2015, A new *Synlestidae* damselfly (Insecta: Odonata: Zygoptera) from the early  
705 Eocene of Nahuel Huapi Este, Patagonia, Argentina: *Arquivos Entomológicos*, v. 14, p. 287-  
706 294.

707 Petrulevičius, J. F., 2016, A new pentatomoid bug from the Ypresian of Patagonia, Argentina: *Acta*  
708 *Palaeontologica Polonica*, v. 61, no. 4, p. 863-868.

709 Petrulevicius, J. F., and Nel, A., 2013, A new *Frenguelliidae* (Insecta: Odonata) from the early Eocene  
710 of Laguna del Hunco, Patagonia, Argentina: *Zootaxa*, v. 3616, no. 6, p. 597-600.

711 Rapela, C.W., Spalletti, L.A., Merodio, J.C., and Aragón, E., 1984, El vulcanismo Paleoceno – Eoceno  
712 de la provincial volcánica Andino - Patagónica: *Actas 9º Congreso Geológico Argentino*, no. 1,  
713 p. 189-213.

714 Rapela, C. W., Spalletti, L. A., Merodio, J. C., and Aragón, E., 1988, Temporal evolution and spatial variation of early  
715 Tertiary volcanism in the Patagonian Andes (40° S-42°30' S): *Journal of South American Earth Sciences*, v. 1, p.  
716 75-88.

717 Reguero, M. A., Gelfo, J. N., López, G. M., Bond, M., Abello, A., Santillana, S. N., and Marenssi, S.  
718 A., 2014, Final Gondwana breakup: the Paleogene South American native ungulates and the  
719 demise of the South America–Antarctica land connection: *Global and Planetary Change*, v.  
720 123B, p. 400-413.

721 Reguero, M., Goin, F., Hospitaleche, C. A., Dutra, T., and Marenssi, S., 2013, Late  
722 Cretaceous/Paleogene West Antarctica terrestrial biota and its intercontinental affinities,  
723 Dordrecht, Springer, *Springer Briefs in Earth System Sciences*.

724 Reguero, M.A., Marenssi, S.A., and Santillana, S.N., 2002, Antarctic peninsula and South America  
725 (Patagonia) Paleogene terrestrial faunas and environments: biogeographic relationships:  
726 *Paleogeography, Palaeoclimatology, Palaeoecology*, v. 179, p. 189-210.

727 Renne, P., Swisher, C., Deino, A., Karner, D., Owens, T., and DePaola, D., 1998, Intercalibration of  
728 standards, absolute ages and Uncertainties in  $40\text{Ar}/39\text{Ar}$  dating: *Chemical Geology*, v. 145, p.  
729 117-152.

730 Renne, P.R., 2000, K-Ar and  $40\text{Ar}/39\text{Ar}$  Dating in Quaternary Geochronology: Methods and  
731 Applications, in Noller, J.S., Sowers, J.M., and Lettis, W.R., eds., *American Geophysical*  
732 *Union Reference Shelf Series* v. 4, p. 77-100.

733 Romero, E. J., and Hickey, L. J., 1976, A fossil leaf of Akaniaceae from Paleocene beds in Argentina:  
734 *Bulletin of the Torrey Botanical Club*, v. 103, no. 3, p. 126-131.

735 Romero, E. J., Dibbern, M. C., and Gandolfo, M. A., 1988, Revisión de *Lomatia bivascularis* (Berry)  
736 *Frenguelli* (Proteaceae) del yacimiento de la Laguna del Hunco (Paleoceno), Pcia. del Chubut:

737 Actas del IV Congreso Argentino de Paleontología y Bioestratigrafía, Mendoza, v. 3, p. 125-  
738 130.

739 Salgado, L., 2007, Patagonia and the study of its Mesozoic reptiles: a brief history, in Gasparini, Z.,  
740 Salgado, L., and Coria, R. A., eds., Patagonian Mesozoic Reptiles: Bloomington, Indiana,  
741 Indiana University Press, p. 1-28.

742 Simpson, G. G., 1935, Occurrence and relationships of the Río Chico fauna of Patagonia: American  
743 Museum Novitates, v. 818, p. 1-21.

744 Simpson, G. G., 1950, History of the fauna of Latin America: American Scientist, v. 38, no. 3, p. 361-  
745 389.

746 Simpson, G. G., 1980, Splendid Isolation: the Curious History of South American Mammals, New  
747 Haven, Yale University Press.

748 Singer, B.S., Jicha, B.R., Mochizuki, N. and Coe, R.S., 2019. Synchronizing volcanic, sedimentary,  
749 and ice core records of Earth's last magnetic polarity reversal. *Science advances*, 5(8),  
750 p.eaaw4621.

751 Smith, M.E., Singer, B., and Carroll, A., 2003,  $^{40}\text{Ar}/^{39}\text{Ar}$  geochronology of the Eocene Green River  
752 Formation Wyoming: *GSA Bulletin*, v.15, p. 540-565.

753 Smith, M.E., Singer, B., Carroll, A.R., and Fournelle, J.L., 2006, High-resolution calibration of Eocene  
754 strata:  $^{40}\text{Ar}/^{39}\text{Ar}$  geochronology of biotite in the Green River Formation: *Geology*, v. 34, p. 392-  
755 396.

756 Tejedor, M. F., Czaplewski, N. J., Goin, F. J., and Aragón, E., 2005, The oldest record of South  
757 American bats: *Journal of Vertebrate Paleontology*, v. 25, p. 990-993.

758 Tejedor, M. F., Goin, F. J., Gelfo, J. N., López, G., Bond, M., Carlini, A. A., Scillato-Yané, G. J.,  
759 Woodburne, M. O., Chornogubsky, L., Aragón, E., Reguero, M. A., Czaplewski, N. J., Vincon,  
760 S., Martin, G. M., and Ciancio, M. R., 2009, New early Eocene mammalian fauna from western  
761 Patagonia, Argentina: *American Museum Novitates*, v. 3638, p. 1-43.

762 Wilf, P., 2012, Rainforest conifers of Eocene Patagonia: attached cones and foliage of the extant  
763 Southeast Asian and Australasian genus *Dacrycarpus* (Podocarpaceae): *American Journal of*  
764 *Botany*, v. 99, no. 3, p. 562-584.

765 Wilf, P., Carvalho, M. R., Gandolfo, M. A., and Cúneo, N. R., 2017, Eocene lantern fruits from  
766 Gondwanan Patagonia and the early origins of Solanaceae: *Science*, v. 355, no. 6320, p. 71-75.

767 Wilf, P., and Escapa, I. H., 2015, Green Web or megabiased clock? Patagonian plant fossils speak on  
768 evolutionary radiations: *New Phytologist*, v. 207, no. 2, p. 283-290.

769 Wilf, P., Cúneo, N. R., Escapa, I. H., Pol, D., and Woodburne, M. O., 2013, Splendid and seldom  
770 isolated: the paleobiogeography of Patagonia: *Annual Review of Earth and Planetary Sciences*,  
771 v. 41, p. 561-603.

772 Wilf, P., Cúneo, N. R., Johnson, K. R., Hicks, J. F., Wing, S. L., and Obradovich, J. D., 2003, High  
773 plant diversity in Eocene South America: evidence from Patagonia: *Science*, v. 300, no. 5616,  
774 p. 122-125.

775 Wilf, P., Escapa, I. H., Cúneo, N. R., Kooyman, R. M., Johnson, K. R., and Iglesias, A., 2014, First  
776 South American *Agathis* (Araucariaceae), Eocene of Patagonia: *American Journal of Botany*, v.  
777 101, no. 1, p. 156-179.

778 Wilf, P., Johnson, K. R., Cúneo, N. R., Smith, M. E., Singer, and B. S., Gandolfo, M. A., 2005, Eocene  
779 plant diversity at Laguna del Hunco and Rio Pichileufu, Patagonia, Argentina: *The American*  
780 *Naturalist*, v. 165, p. 634-650.

781 Wilf, P., Labandeira, C. C., Johnson, K. R., and Cúneo, N. R., 2005b, Richness of plant-insect  
782 associations in Eocene Patagonia: a legacy for South American biodiversity: *Proceedings of the*  
783 *National Academy of Sciences USA*, v. 102, no. 25, p. 8944-8948.

784 Wilf, P., Little, S. A., Iglesias, A., Zamaloa, M. C., Gandolfo, M. A., Cúneo, N. R., and Johnson, K. R.,  
785 2009, *Papuacedrus* (Cupressaceae) in Eocene Patagonia: a new fossil link to Australasian  
786 rainforests: American Journal of Botany, v. 96, no. 11, p. 2031-2047.

787 Wilf, P., Nixon, K. C., Gandolfo, M. A., and Cúneo, N. R., 2019, Eocene Fagaceae from Patagonia and  
788 Gondwanan legacy in Asian rainforests: Science, v. 364, no. 6444, eaaw5139.

789 Wilf, P., Singer, B. S., Zamaloa, M. C., Johnson, K. R., and Cúneo, N. R., 2010, Early Eocene  
790  $^{40}\text{Ar}/^{39}\text{Ar}$  age for the Pampa de Jones plant, frog, and insect biota (Huitrera Formation, Neuquén  
791 Province, Patagonia, Argentina): Ameghiniana, v. 47, no. 2, p. 207-216.

792 Woodburne, M.O., Goin, F.J., Bond, M. Carlini, A.A., Gelfo, G.M.L., Iglesias, A., and Zemicz, A.N.,  
793 2014a, Paleogene Land Mammal Faunas of South America; a Response to Global  
794 Climatic Changes and Indigenous Floral DiversityJournal of Mammalian Evolution, v.  
795 21, p. 1-73. doi:10.1007/s10914-012-9222-1

796 Woodburne, M. O., Goin, F. J., Raigemborn, M. S., Heizler, M., Gelfo, J. N., and Oliveira, E. V.,  
797 2014b, Revised timing of the South American early Paleogene Land Mammal Ages: Journal of  
798 South American Earth Sciences, v. 54, p. 109-119.

799

800 Zachos, J. C., Dickens, G. R., and Zeebe, R. E., 2008, An early Cenozoic perspective on greenhouse  
801 warming and carbon-cycle dynamics: Nature, v. 451, no. 7176, p. 279-283.

802

803  
804

## 805 FIGURE CAPTIONS

806 Figure 1: Simplified geologic map of the study area, modified from Aragón and Mazzoni, (1997), and  
807 sampling localities. La Barda locality is off the map, approximately 6 km distant from the Laguna Fría  
808 locality on a 192° bearing (Tejedor et al., 2009). Solid lines represent observed boundaries from field  
809 work and satellite imagery. Dashed lines represent inferred boundaries. The resurgent dome area has  
810 not yet been mapped out in detail but contains pyroclastic deposits of the Tufolitas del Hunco; intra-  
811 caldera volcanic flows and dikes; and capping Miocene to Pleistocene basalt flows.

812

813 Figure 2: Cross-sectional cartoon across southern portion of Middle Chubut River Pyroclastic Volcanic  
814 Complex. Key fossil sites and rock units with age determinations are emphasized. Figure is not to scale. See  
815 Figure 1 for correct spatial distances between localities. Age determinations cited from Wilf et al., (2003 and  
816 2005) have been adjusted to more recent standard of Kuiper et al., 2008.

817

818 Figure 3: Field photographs of fossil-bearing lithofacies. A. Overview of the Tufolitas Laguna del  
819 Hunco (Laguna del Hunco locality). B. Laminated mudstone facies (Laguna del Hunco locality). C.  
820 Photomicrograph of organic-rich laminated mudstone facies ((Laguna del Hunco locality). D. Gray  
821 ashy mudstone overlain by sediment gravity flow (resistant bed; Laguna del Hunco locality). E.  
822 Photomicrograph showing microcrystalline nature of the gray ashy mudstone facies (Laguna del Hunco  
823 locality). F. Leaf fossil preserved in gray ashy mudstone (Laguna del Hunco locality). G. Volcaniclastic  
824 turbidite showing all 5 Bouma subdivisions (Laguna del Hunco locality). H. Glass dome intruding gray  
825 ashy mudstone facies (Central Caldera locality). I. Petrified tree trunk preserved in a clast-rich ash-flow  
826 tuff (Escuela Piedra Parada locality). J. Root cast and cross-bedding in a crystal-rich reworked  
827 pyroclastic facies (Laguna Fría locality). K. Field relationships between the Ignimbrita Barda  
828 Colorada, valley-filling volcaniclastic facies, orange gnimbrite, and Laguna Fría capping basalt  
829 (Laguna Fría locality). Fossil locality lies stratigraphically above the orange ignimbrite and below the  
830 basalt. L. Oblique composite satellite image looking east at the area between the Laguna Fría and La  
831 Barda faunal localities (3x vertical exaggeration. Image © 2019 CNES / Airbus, © 2018 Google,  
832 Image © 2019 Maxar Technologies)

833

834 Figure 4: Schematic block diagrams of depositional environments interpreted in this study. Scale bars are  
835 approximate horizontal distances. Vertical scale is exaggerated. Localities are in **bold**. Flora/Fauna and facies  
836 names are (in brackets).

837

838 Figure 5: Summary of  $^{40}\text{Ar}/^{39}\text{Ar}$  dates from sanidine and plagioclase in Laguna Fría Orange Ignimbrite, Southern  
839 Ignimbrite, and Upper Ignimbrita Barda Colorada. Inverse isochron diagrams for the Southern Ignimbrite and  
840 Laguna Fría Orange Ignimbrite display intercepts which diverge from atmospheric values, and so the isochron  
841 age is preferred in both cases. Open points indicate analyses excluded from weighted mean age calculations.  
842 Weighted mean ages are shown with  $2\sigma$  uncertainties, whereas individual analyses are shown with  $1\sigma$

843   uncertainties. The isochron age of the Laguna Fría Capping Basalt is denoted by a dashed line, with  $2\sigma$   
844   uncertainties indicated by a gray band.

845

846   Figure 6. Age spectrum and inverse isochron diagrams illustrating results of an  $^{40}\text{Ar}/^{39}\text{Ar}$  incremental heating  
847   experiment on groundmass from the Laguna Fría Capping Basalt. Steps excluded from analysis are show as open  
848   boxes.

849

850   Figure 7: Summary of Eocene age relationships and terrestrial fauna and flora. Modified from Krause  
851   et al. (2017) and Wilf (2012) based on new results from the Piedra Parada caldera (reported in this  
852   study). Age determinations based on  $^{40}\text{Ar}/^{39}\text{Ar}$  and have been adjusted to decay constants of Kuiper et  
853   al., (2008). Shaded boxes indicate potential age range for each fossil assemblage, taking into account  
854    $2\sigma$  errors.

855

856   **Footnote to be inserted at bottom of page for line 164:**

857   <sup>1</sup> GSA Data Repository item 0000000, Full documentation of  $^{40}\text{Ar}/^{39}\text{Ar}$  geochronology, is available at  
858   <http://www.geosociety.org/pubs/ft2012.htm> or by request to [editing@geosociety.org](mailto:editing@geosociety.org).

859

# Figure 1

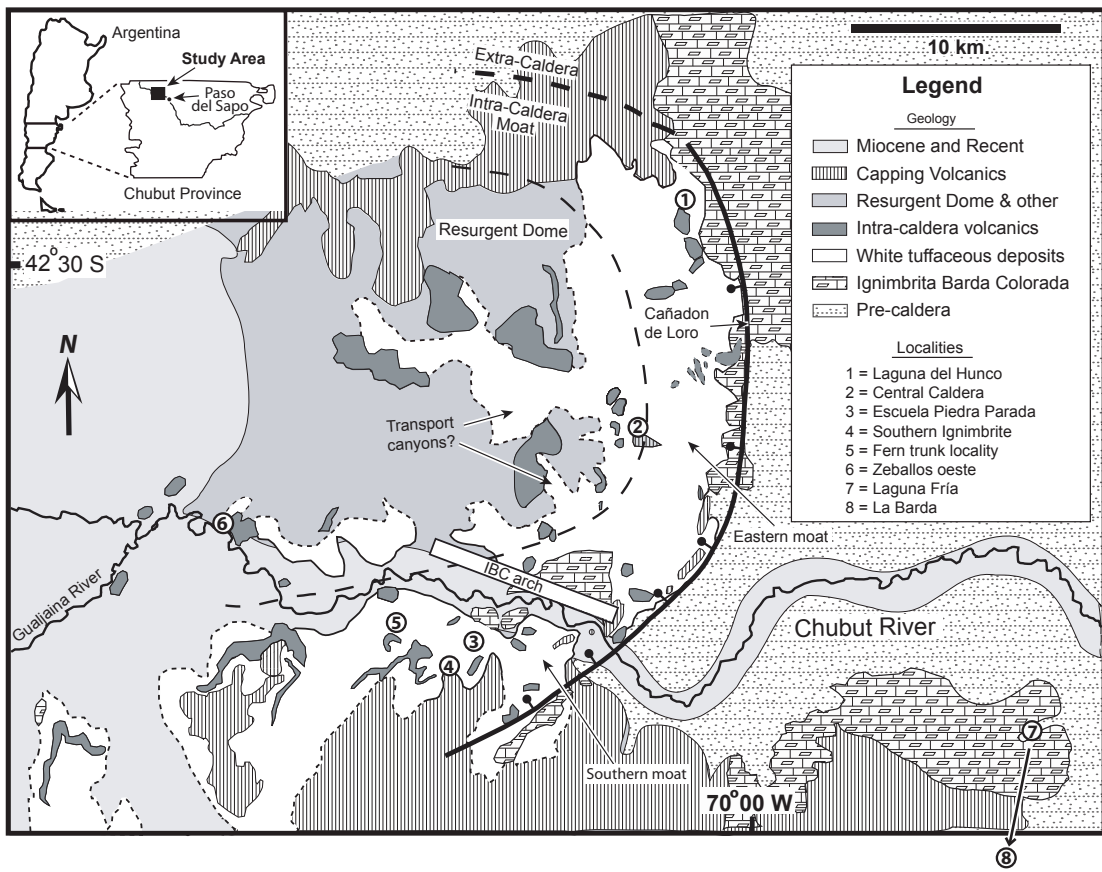


# Figure 1

# Figure 2

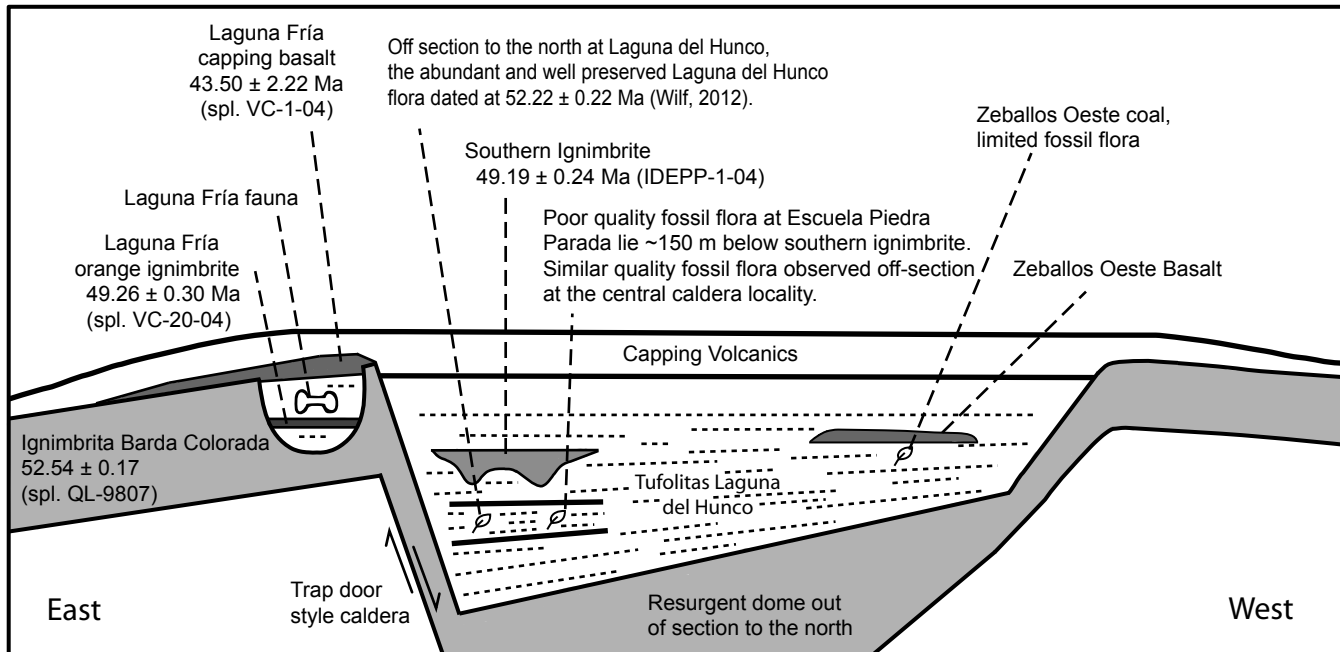


Figure 2

Figure 3, part 1

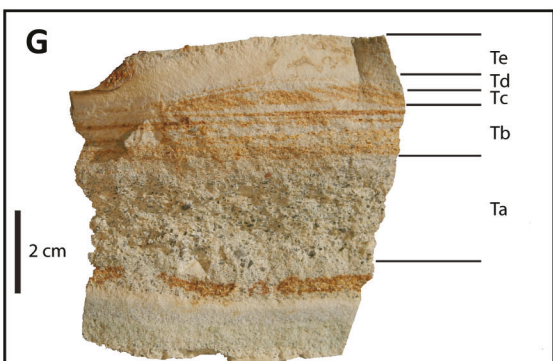
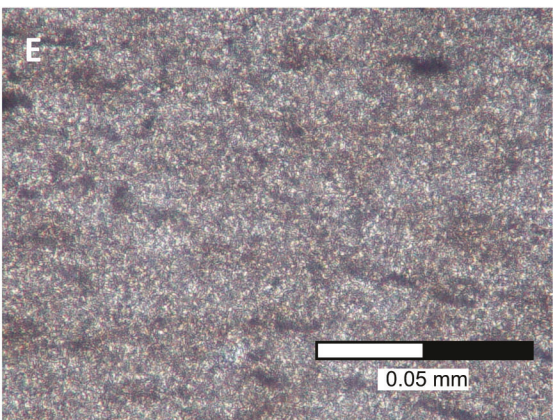
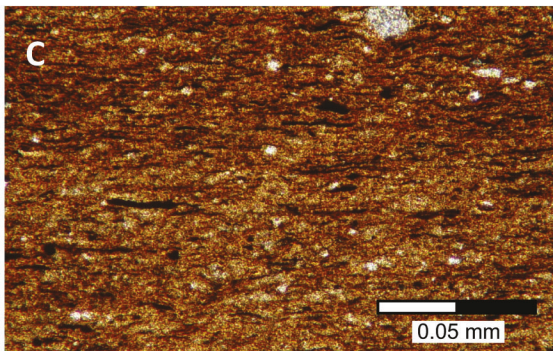


Figure 3

# Figure 3, part 2

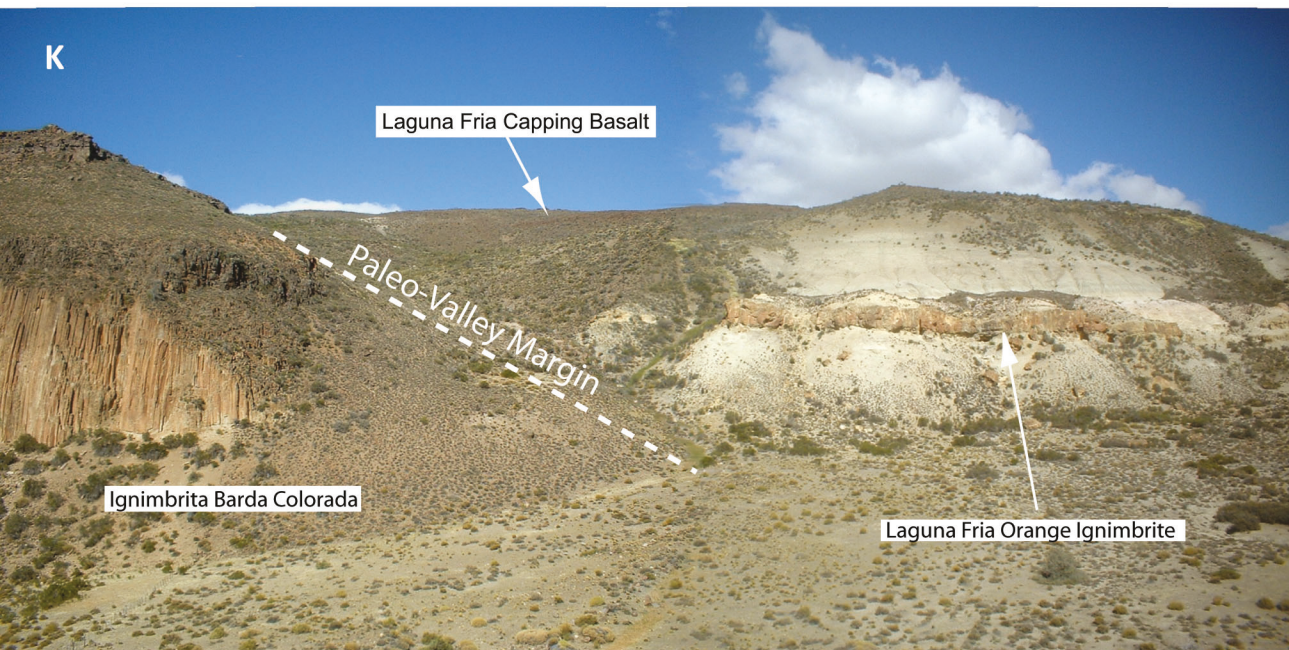
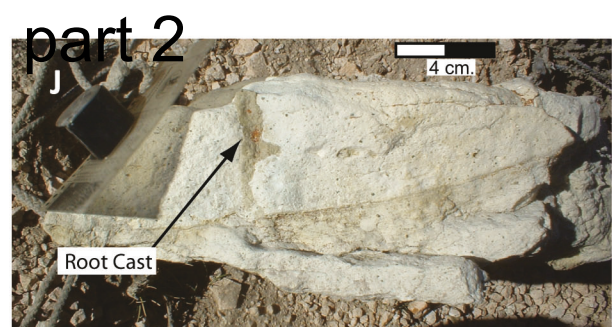
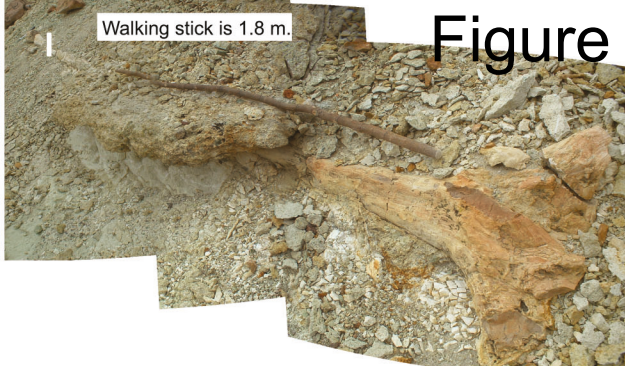
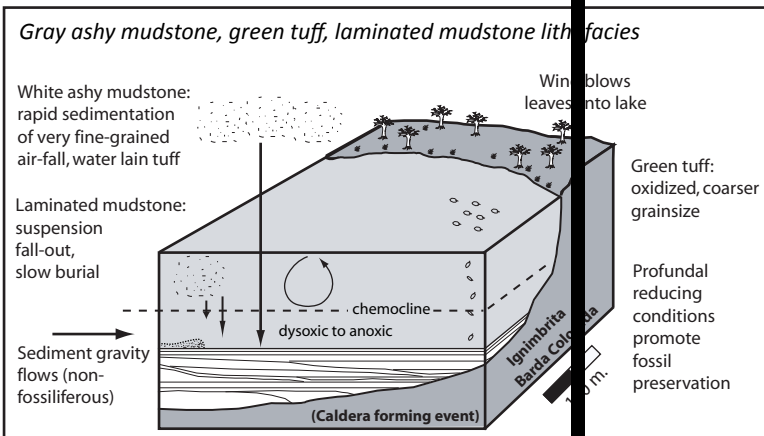


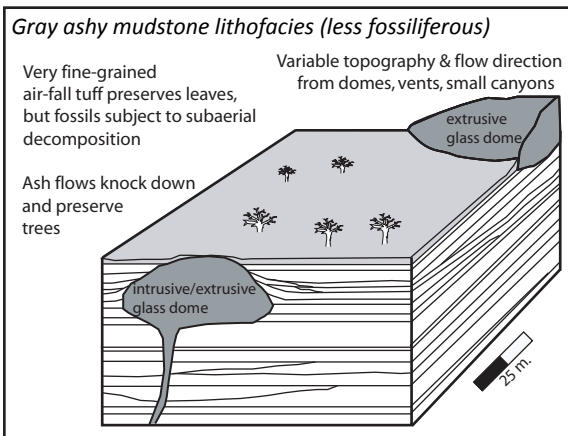
Figure 3 (continued)

# Figure 4

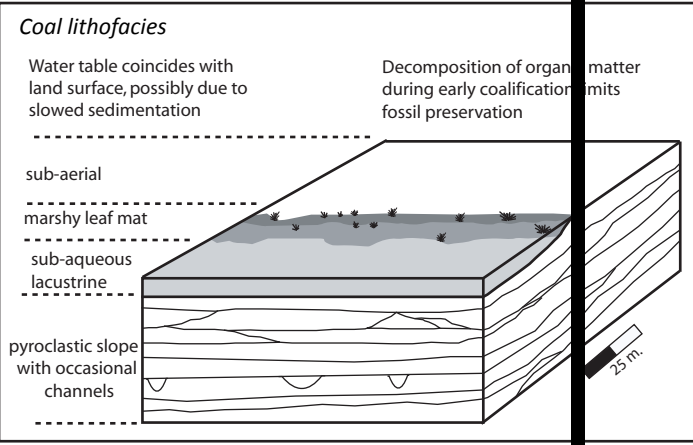
## A. Laguna del Hunco



## B. Escuela Piedra Parada, Central Caldera



## C. Zeballos Oeste



## D. Laguna Fria

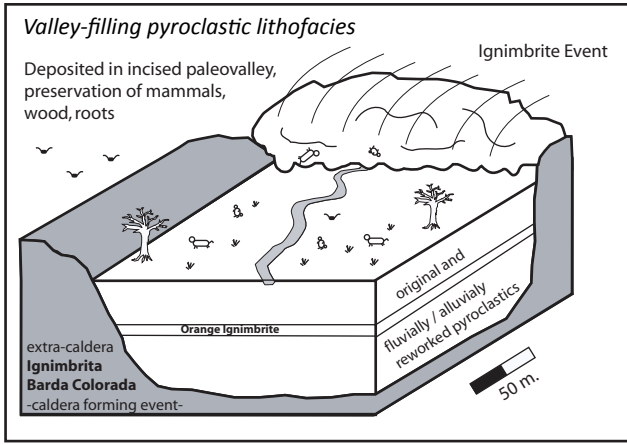
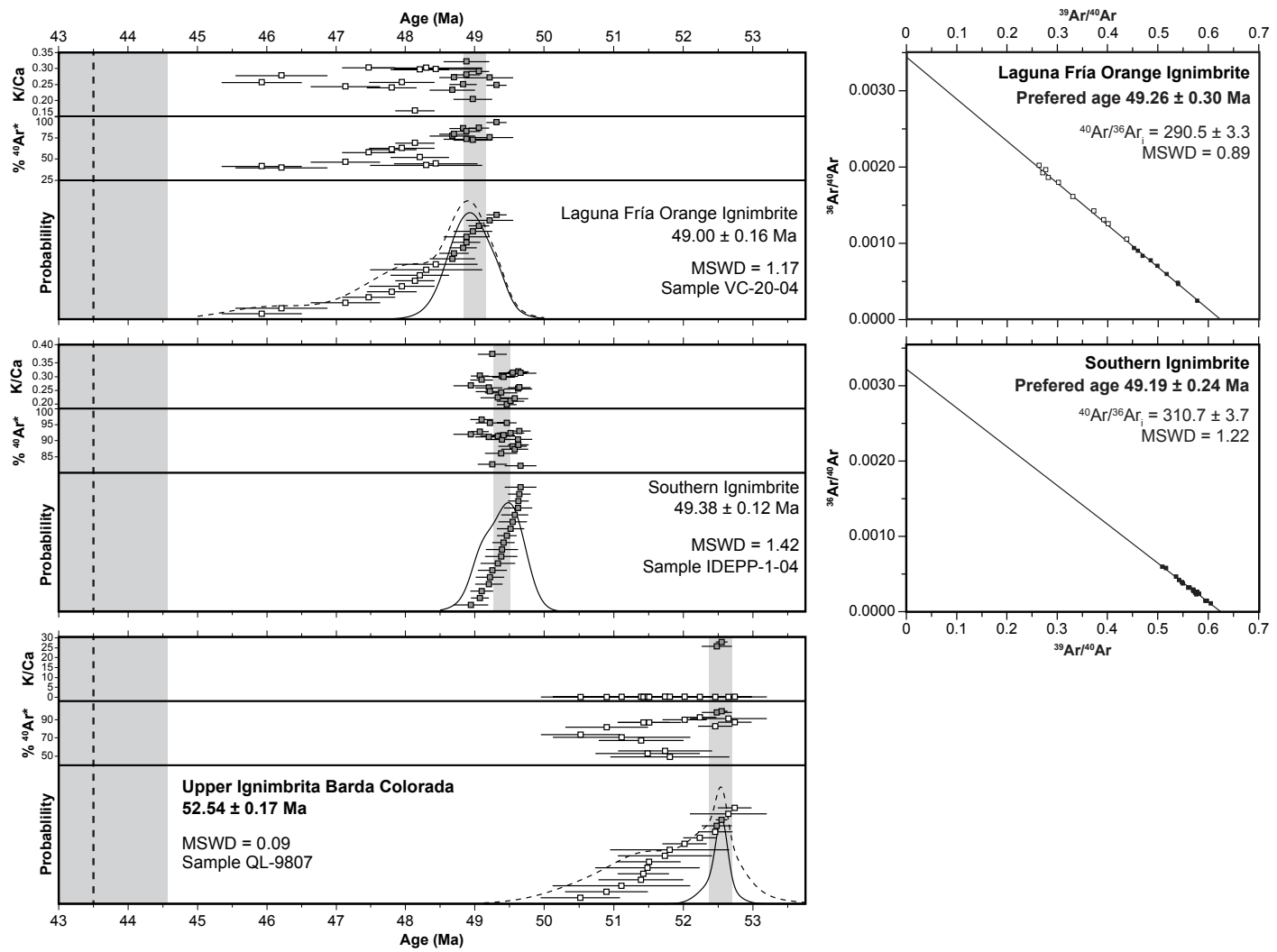


Figure 4

# Figure 5



# Figure 5

# Figure 6

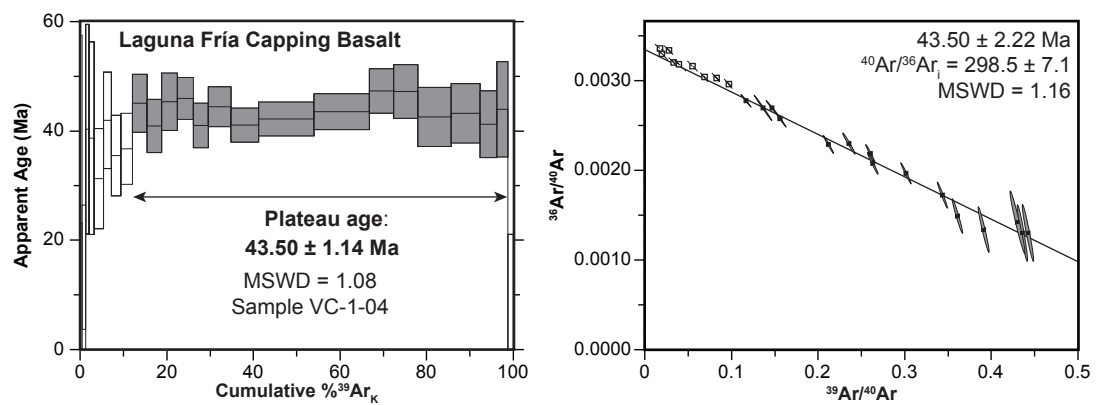


# Figure 6

# Figure 7

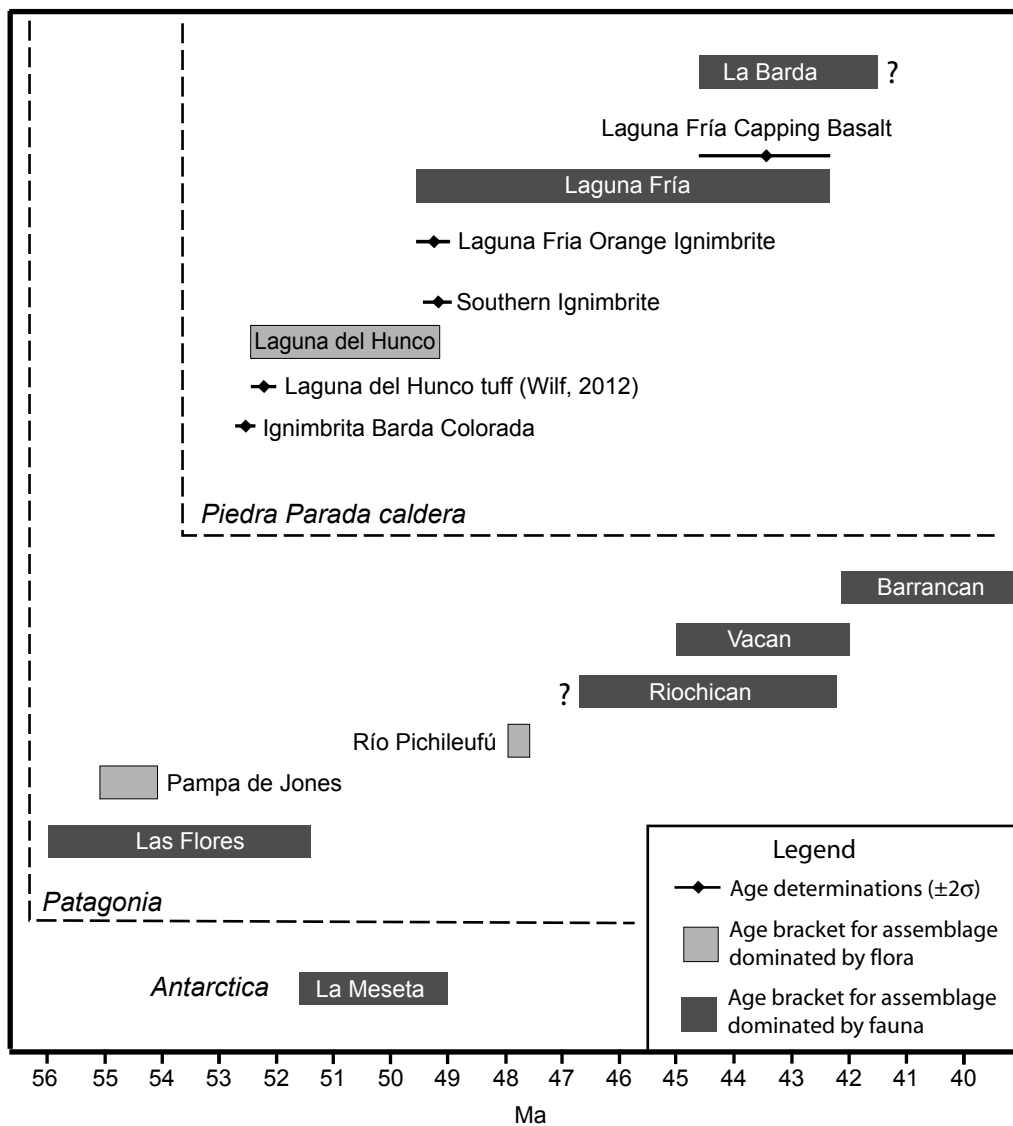


Figure 7

TABLE 1. SUMMARY OF RADIOISOTOPIC AGES

Sample	Unit	Latitude (°S)	Longitude (°W)	Mineral	N	% <sup>39</sup> Ar	MSWD	K/Ca	Plateau Age (Ma)	Isochron Age (Ma)	±2σ	±2σ	( <sup>40</sup> Ar/ <sup>36</sup> Ar) <sub>i</sub>	±2σ
<u>Incremental Heating Results</u>														
VC-1-04	Laguna Fria Basalt	42.72447	69.84536	Plag	15/24	86.6	1.08	0.0	<b>43.50</b>	<b>1.14</b>	43.50	2.22	298.54	7.05
<u>Single Crystal Laser Fusion Results</u>														
VC-20-04	Orange Ignimbrite	42.72447	69.84536	Plag	9/19		1.17	0.3	49.00	0.16	<b>49.26</b>	<b>0.30</b>	290.5	3.3
IDEPP-1-04	Southern Ignimbrite	42.68194	70.16803	Plag	18/18		1.42	0.3	49.38	0.10	<b>49.19</b>	<b>0.24</b>	310.7	3.7
QL-9807	Upper Ignimbrite Barda Colorado	42.72447	69.84536	San	2/16		0.09	27.3	<b>52.54</b>	<b>0.17</b>	N.D.	N.D.	N.D.	N.D.

*Note:* Bold font indicates preferred ages. Ages calculated relative to Fish Canyon sanidine interlaboratory standard at 28.201 Ma (Kuiper et al. 2008). Age uncertainty includes analytical uncertainty + J uncertainty. Decay constants and isotopic abundances after Min et al. (2000).